National University of Lesotho

Determination of Cost-Reflective Feed-in Tariff for Grid Connected Solar PV Systems in Lesotho

Limpho Kokome

A dissertation submitted in partial fulfilment of
the requirements for the degree of

Master of Science in Sustainable Energy

Offered by the

Energy Research Centre
Faculty of Science & Technology

May 2020

ABSTRACT

Lesotho needs a feed-in tariff policy that can help accelerate integration of renewable energy in its electricity grid. In this study a method to determine the feed-in tariff for grid connected solar Photovoltaic (PV) systems was developed. The necessity to set different tariffs for different locations in terms of the solar PV array yield □ , and different tariffs for different installed capacities were examined. Location specific tariffs were examined because given a particular solar module, the array yield □ could vary with location because of different ambient temperature and radiation, while size specific tariffs were examined because solar PV systems have different specific costs for different system sizes. In order to determine the cost reflective feed-in tariff, the Levelized Cost of Electricity (LCOE) was used as the objective function. With this approach the feed-in tariff was set as the price for selling electricity that is reasonably above the unit cost of production. A custom spreadsheet model was used to calculate the solar PV array yield □ over Lesotho. This array yield was used to divide Lesotho into two regions, low yield regions, and high yield regions. Representative systems were chosen and the feed-in tariff for different solar PV installed capacities in both regions were determined. The study found that the feed-in tariff varies with location and system size as follows;

System Category	FiT ($/kWh)	
	Low Array Yield Region	High Array Yield Region
30 kWp Roof Mount	0.1778	0.1616
500 kWp Roof Mount	0.1597	0.1451
30 kWp Ground Mount	0.1740	0.1581
500 kWp Groun Mount	0.1453	0.1321
10 000 kWp Ground Mount	0.1138	0.1034

The study recommends a feed-in tariff that is both location and size specific. The feed-in tariff depends on duration of the tariff with shorter periods resulting in higher feed-in tariff. A 20-year duration of the feed-in tariff is therefore recommended by this study. The method used in this study to determine the feed-in tariff included the impact of inflation in the analysis and therefore a fixed feed-in tariff (that is not indexed to inflation) is recommended. The energy regulator, and the ministry responsible for energy policy setting can make use of this study in setting out feed-in tariff policy.

Symbols and Acronyms

FiT	Feed in Tariff
G_{sc}	Solar Constant
GWp	Gigawatt peak. Units of electrical energy
I_T	Total Radiation Incident on a Tilted Surface
$I_{T,b}$	Beam Radiation Incident on a Tilted Surface
$I_{T,d}$	Diffuse Radiation Incident on a Tilted Surface
$I_{T,r}$	Reflected Radiation Incident on a Tilted Surface
IEA	International Energy Agency
IPP	Independent Power Producer
IRR	Internal Rate of Return
kWh	Kilowatt-hour
L_c	Collection Losses
L_s	System Losses
LCOE	Levelized Cost of Electricity
LEC	Lesotho Electricity Company
LEWA	Lesotho Electricity and Water Authority
LHDA	Lesotho Highlands Development Authority
MPPT	Maximum Power Point Tracker
MW	MegaWatt
N	Day number in a year
NERSA	National Energy Regulator of South Africa
NPV	Net Present Value
NREL	National Renewable Energy Laboratory
PPA	Power Purchase Agreement
PR	Performance Ratio
PV	Photovoltaic
SADC	Southern African Development Community
STC	Standard Test Conditions
T_a	Ambient Temperature
T_c	Cell Operating Temperature
WACC	Weighted Average Cost of Capital
Y_R	Reference Yield
Y_A	Array Yield
Y_F	Final Yield

Table of Contents

1. INTRODUCTION 1

1.1. Background 1

1.2. Problem Statement 3

1.3. Aim and Objectives 4

1.4. Justification 4

1.5. Research Question 4

1.6. Organization of the Paper 5

2. LITERATURE REVIEW 5

2.1. Defining FiT 5

2.2. Tariff Design Options 9

2.3. Review of Solar PV Costs 12

2.4. Radiation Received on a Tilted Collector 17

2.5. Solar Energy Output 24

2.6. Performance Indices 28

2.7. Bilinear Interpolation 30

3. MATERIALS AND METHODS 31

3.1. Data Used 31

3.2. Gridding 31

3.3. Determination of Incident Radiation 32

3.4. Determination of Energy Output 33

3.5. Bilinear Interpolation 37

3.6. Zoning 37

3.7. Determination of Feed-In-Tariff 38

4. RESULTS....45
4.1. Performance Indicators....45
4.2. Zoning....46
4.3. Financial Results....47
5. DISCUSSION....55
5.1. Policy Implications....55
5.2. Limitations....55
6. CONCLUSIONS AND RECOMMENDATIONS....55
7. REFERENCES....57

List of Tables

Table 1-1: Electricity Generating Units in Lesotho 1
Table 2-1: 2009 vs 2011 ReFIT Rates in South Africa 8
Table 2-2: Installed Costs for Q1 2018 in the US 14
Table 2-3: 2010 & 2018 LCOE ranges for Solar PV systems in the US 16
Table 2-4: Irradiance coefficients for Perez Model 23
Table 3-1: Modelled System Capacities 35
Table 3-2: Specifications for Canadian Solar Superpower CS6K 300MS 36
Table 3-3: Specifications for KACO Powador 60.0 TL 37
Table 3-4: Assumed Interest Rates 45
Table 3-5: Breakdown of Installed Costs..... 46
Table 3-6: Economic and Financial Assumptions 46
Table 4-1: Results for Performance Indicators 47
Table 4-2: Table of Array and Final Yields for High and Low Yield Regions 49
Table 4-3: Results for FiT 49
Table 6-1: Recommended FiT for Grid Connected Solar PV Systems 58

List of Figures

Figure 2-1: Global Growth of FiT by Country Type 7
Figure 2-2: Global Weighted Average Installed Costs for Solar PV 13
Figure 2-3: Global Weighted Average LCOE 14
Figure 2-4: Installed Costs for solar PV Systems from 2010 to 2018 in the US 15
Figure 2-5: Sensitivity of LCOE to Input Parameters 16
Figure 2-6: O&M Costs for Residential, Commercial and Utility Scale PV Systems 17
Figure 2-7: Representation of Solar Geometric Angles;..... 19
Figure 2-8: Global impact of soiling 27
Figure 2-9: Histogram of Annual Degradation Rates 28
Figure 2-10: A Figure of Reference, Array and Final Yields, ... 29

Figure 2-11: Bilinear interpolation in and (x,y) grid 31
Figure 3-1: Inverter Efficiency from Datasheet 38
Figure 3-2: Modelled Inverter Efficiency 38
Figure 3-3: Illustration of the Internal Rate of Return 44
Figure 4-1: Map of Annual Array Yield, Y_A for Lesotho 48
Figure 4-2: Cash flows for the Project for Utility Scale Systems 50
Figure 4-3: Cash flows for Equity for Utility Scale Systems 50
Figure 4-4: Cash flow for Project for Commercial Scale Systems 51
Figure 4-5:Cash flows for Equity for Commercial Scale Systems 52
Figure 4-6:Cash flow for Project for Commercial Scale Systems 53
Figure 4-7: Cash flows for Equity for Commercial Scale Systems 53
Figure 4-8:Cash flow for the Project in Roof Mount Residential Scale Systems 54
Figure 4-9: Cash flows for Equity in the Roof Mount Residential Scale Systems 55
Figure 4-10: Cash flow for Project in the Ground Mount Residential Scale Systems 56
Figure 4-11: Cash flow for Equity in the Ground Mount Residential Scale Systems 56

Acknowledgements

First I wish to acknowledge my supervisor Engineer Tawanda Hove for the immense contribution that he has made as a supervisor in carrying out this mammoth task. Secondly I wish to acknowledge Mr. Thuso Ntlama from the Lesotho Water and Electricity Authority for allowing me the opportunity to consult. Lastly I wish to acknowledge my family and friends who were very supportive during a tough 2019.

1. INTRODUCTION

1.1. Background

In 2018 Lesotho had a 24% electricity base load deficit and a 44% peak load deficit [1]. The generation capacity has stood at 74.7 MW since 1998 [2]. This while evidence shows that electricity demand has far outgrown the current generation capacity. For example the peak demand in 2015 was 155 MW, and 177.31 MW in 2019 [1], [2]. The electricity industry in Lesotho is dominated by two entities, the Lesotho Electricity Company (LEC) which is the transmitter and distributor of electricity, and the Lesotho Highlands Development Authority (LHDA) the main electricity generator through 'Muela Hydropower Plant [3]. Besides the 'Muela Hydropower Plant, there are other considerable electricity generating units that contribute to local electricity generation. The generating units have been shown in Table 1-1 [4]

Table 1-1: Electricity Generating Units in Lesotho

Place of Installation	Technology	Capacity (MW)
'Muela	Hydropower	72
Semonkong	Hydropower	0.18
Mantsonyane	Hydropower	2
Moshoeshoe 1 International Airport	Solar Power	0.28

Adoption of solar power has been touted as one of the means by which local electricity generation can be increased to decrease the capacity shortage [3].

A solar photovoltaic (PV) grid tie system consists of solar modules, junction boxes and an inverter that is connected to the electricity grid [5]. The global installed capacity of grid tie solar PV systems reached 100 GWp in 2012, with Europe being the leader in installed capacity representing 71% of these installations, and Asia Pacific at 15.8% [6]. 94 GWp of capacity was added to the global capacity in 2015 alone, highlighting the fast growth of solar PV installations [7]. The main driver of this trend is mostly attributed to the implementation of Feed-in Tariff policy (FiT) [6]. Another driver of this trend has been the cost of electricity produced from solar PV, which has dropped significantly in the past two decades mainly driven by falling prices and increased efficiency of solar modules, as well as advanced research in semiconductor technology [8].

Between 2010 and 2016, the Levelized Cost of Electricity (LCOE) fell by more than 60% across the world [9]. From 2017 to 2018 the weighted average LCOE fell by 13%, which saw a 77% decline in LCOE from 2010 to 2018 [7].

1.1.1. Overview of Efforts to accelerate adoption of Renewable Energy in Lesotho

Some efforts have been made in Lesotho to increase the share of renewable energy in the energy mix. Some of these efforts include the 2015 publication of the Lesotho Energy Policy 2015-2025 which includes policy statements on adoption of renewable energy. In 2015 a call for expression of interest was released by the Department of Energy to construct, own and operate a 20 MWp solar power plant, and negotiate a Power Purchase Agreement (PPA) with LEC. Further to these efforts, a consultant was engaged to compile an Independent Power Producer (IPP) framework by the Lesotho Electricity and Water Authority 2015 [10]. These efforts will now be discussed in detail below;

Lesotho Energy Policy 2015-2025: The energy policy was published in 2015 by the Department of Energy, under the Ministry of Energy and Meteorology. With regard to renewable energy, the objectives of the policy are to improve energy security by cutting down on fossil fuels and electricity that are bought from abroad, to increase access to modern energy services especially in rural areas, to reduce emissions in the energy sector [11]. The policy aims at the following [11];

- To develop PPA and IPP frameworks that would allow participation of private developers in electricity generation,
- to ensure guaranteed access or priority rule for electricity generation units, 500kW or less in capacity, to connect at low voltage and
- to develop a cost-reflective pricing mechanism that will ensure financial sustainability and promote investment by private developers in the energy sector.

In Section 2.2 the importance of the priority rule and a price setting mechanism for electricity generating units are discussed as options for the Feet-in Tariff (FiT) policy.

2015 Call for Interest of Expressions: In 2015 the Department of Energy released a call for expression of interest for developers to construct, own and operate a 20 MW solar PV plant and negotiate a PPA with the Lesotho Electricity Company. In 2016 the project was awarded to One Power Lesotho which plans to construct the facility in Mafeteng district [12].

2015 Independent Power Producer Framework: The Lesotho Electricity and Water Authority (LEWA) engaged a consultant in 2015 to develop an IPP framework. The objectives of the assignment were as follows [13];

- to develop an IPP framework and related legal instruments within the renewable energy arena,
- to develop a comprehensive financial and economic model for determining renewable energy feed-in tariff,
- to develop a PPA template that can be used by private developers or IPPs in negotiation with the off taker,
- to develop licensing documents for different types of generating units, to develop guidelines for the development of power.

There are several renewable energy resources in Lesotho, like hydro and wind, however the focus of this study is solar PV.

1.2. Problem Statement

Lesotho's electricity demand far exceeds its local generation capacity. As outlined by LEWA's 2018-2019 annual report, Lesotho's peak electricity demand reached 177.31 MW within this reporting period, while the local generation capacity at 'Muela stayed at 74.7 MW [2]. In order to meet the capacity shortage Lesotho imports electricity from South Africa and Mozambique [2]. In 2008 Lesotho experienced blackouts which were reportedly caused by the fact that 'Muela Hydropower Plant did not meet Lesotho's Electricity demand, and that South Africa's electricity utility company, Eskom was cutting power in order to meet a balance of power demand and supply on their own system [14]. Lesotho has a poor electrification rate at 34%, compared to its Southern African Development Community (SADC) peers; with Eswathini being at 66% and Botswana at 61% [12]. All these can be attributed to lack of sufficient local generation and hence the need for efforts to accelerate adoption of renewable energy. The electricity capacity shortage in Lesotho can be closed by harnessing renewable energy sources, like solar PV but there are several problems facing the energy industry in Lesotho as stipulated below;

- There is no adopted FiT that is calculated on a cost-reflective basis.
- Setting a similar FiT for different locations would lead to developers in regions with poor solar resource being disadvantaged in terms of profitability, while developers in regions with

good solar resource may be overcompensated. Similarly, setting a similar FiT for different capacities would put smaller systems at a disadvantage in terms of profitability because of economies of scale.

1.3.Aim and Objectives

As already mentioned, efforts have been made to accelerate adoption of renewable energy in Lesotho by publishing the Lesotho Energy policy and compiling an IPP framework. The contribution of this study in these efforts is to determine a feed-in tariff for solar PV systems that reflects the costs of construction and operation, while compensating the developers of such systems. Hence the objectives of the study are as follows;

- To prescribe different FiT for different locations and different system sizes
- To determine the FiT for different eligible capacities
- To evaluate the necessity to set different tariffs for different locations and different system sizes

1.4.Justification

The Lesotho Energy Policy 2015 – 2025 includes policy statements and strategies that aim to improve access to renewable energy services. The statements on renewable energy, power generation, tax incentives and Renewable Energy Feed-in-Tariff (ReFIT) are some of the statements aimed at accelerating adoption of renewable energies. However, the policy does not have clear directive and guidance on these topics. The IPP framework, as comprehensive as it may be, still leaves some gaps; it assumes a uniform FiT and hence does not make recommendations on location-specific tariff. These gaps have been found to leave an area of research in determining a FiT for grid-connected solar PV systems, especially on setting different tariffs for different locations based on resource availability. This study is necessary because;

- In Lesotho there is need for policy instruments to accelerate the adoption of renewable energy, particularly solar PV
- There is a need for a feed in tariff that will ensure economic sustainability of solar energy projects, and hence attract private investment in the sector

1.5. Research Question

The objectives of this research have already been mentioned in Section 1.3. This study is expected to provide answers to these research questions;

- What is the suitable FiT for grid connected solar PV systems in Lesotho?
- Should there be different FiT for locations with different available solar resource? Should there be different FiT for different eligible capacities?

1.6.Organization of the Paper

This paper contains six chapters which are organized as follows;

Chapter - 2: Literature Review; In Chapter 2, a literature review has been presented that covers topics under feed-in tariff, its definition and options to consider in the feed-in tariff policy. Solar PV technology has also been reviewed including its costs, how the solar resource is harvested and how its performance is measured.

Chapter - 3: Materials and Methods: In Chapter 3 of the materials and methods, the procedure to determine the feed-in tariff has been defined from both the financial and technical perspectives. The methodology that would aid in determining the necessity for different tariffs for different regions has also been defined.

Chapter – 4: Results: Chapter 4 presents classification of regions based on the determined Annual Array Yield, □ , the results of the determined feed-in tariffs for different regions, and for different types of systems. Performance indices that compare the modelled system for this research with other systems have also been presented in this chapter.

Chapter -5: Discussion: In the discussion section the results have been discussed together with their implications on the existing energy policy and IPP framework. The limitations of this study have also been highlighted in this chapter.

Chapter – 6: Conclusion: The study has been concluded by making recommendation on the tariffs for different yielding regions, classified as low yield and high yield regions. Further recommendations have been made on several tariff design options including location specificity, size specificity, duration of the FiT agreements and inflation indexation. These tariff design options will be covered in more detail Section 2.2.

2. LITERATURE REVIEW

2.1. Defining FiT

Feed-in-Tariff is a policy that is designed and implemented to accelerate the adoption of renewable energy [15], [16]. In the reviewed literature, the definition of FiT circles among four main features

that enable it to achieve its goals; it is a policy that requires an electricity utility to purchase electricity produced from eligible renewable energy sources at a premium price, that is a price higher than the market price of electricity [17]–[20]. The policy guarantees payment for every unit, in kWh or MWh, of electricity fed into the utility grid [16], [17], [19], [21]. The policy specifies the duration of the agreement to purchase electricity from eligible producers typically spanning 15 – 20 years [17]–[20]. Lastly, the policy provides guaranteed access to the grid for renewable energy generating units [16], [22], [23].

FiT was first introduced in Netherlands in 1989, followed by Germany in 1990, Italy in 1992, Denmark in 1993, Spain and Greece in 1994, Latvia in 1998, France in 2000 and Austria in 2002 [19]. Germany is mostly famous for its Renewable Energy Act (EEG) of 2000 through which producers of electricity were paid a fixed rate for the electricity that they fed into the grid for a period of 15 or 20 years [24]–[27]. The country saw an increased share of renewable energy in its electricity generation mix from 6.6% in 2000 to 33.3% in 2017, with the installed capacity of solar PV increasing from 2.9 GWp in 2006 to 42.3 GWp in 2017 [28]. The United Kingdom adopted FiT in April 2010 which resulted in 77.7 MWp newly installed capacity from 28,550 individual systems within one year of its adoption [29]. In China, FiT came into force in July 2011, which grew the installed capacity of solar PV to 77 GWp in 2016 [30]. The importance of FiT in increasing the share of renewable energy in electricity generation mix, particularly solar PV is further emphasized by a case of Japan which started implementation of its first phase of FiT from November 2009. This implementation resulted in the doubled figure of installed solar PV capacity by 2011 to 4.9 GWp. The second phase of the FiT was started in July 2012 for non-residential sector only with the objective to reach between 20% and 35% of electricity from renewables by the end of 2030 [6].

Today FiT is implemented in many countries around the world. In 2012, the number of countries implementing FiT had grown to 66, from less than 5 in 1990 [31]. Some of the notable countries implementing FiT are Germany, Spain, Denmark, Cyprus [32], [33], Australia[34], Japan [6], China [30] and the United Kingdom [29]. Figure 2-1 shows the number of countries that adopted FiT from 1990 to 2012 for both developing and developed country categories;

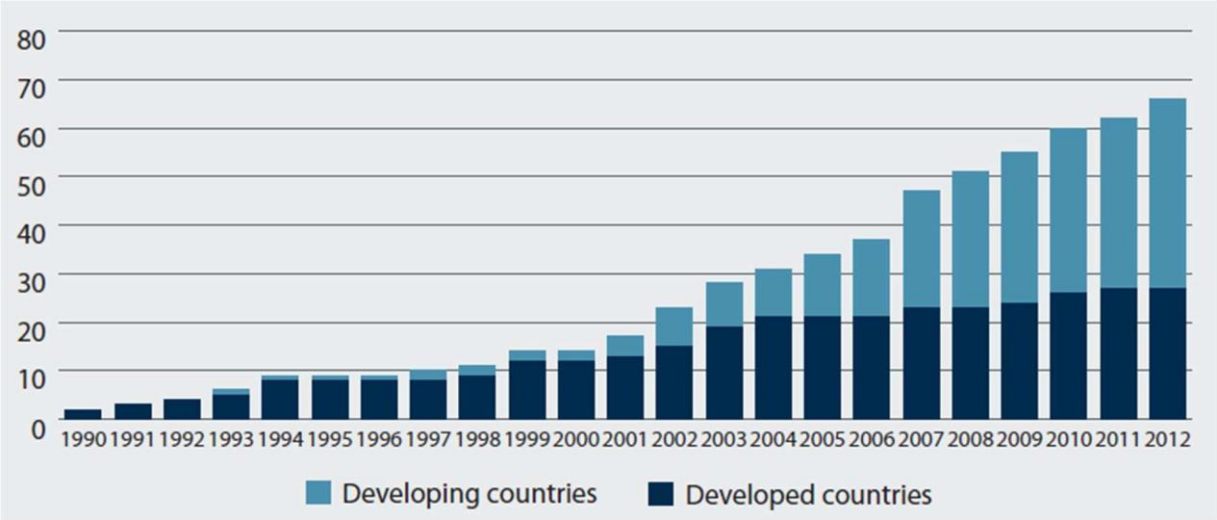

Figure 2-1: Global Growth of FiT by Country Type Source [31]

In Africa, FiT is implemented in Algeria, Kenya, Uganda, Tanzania and Zimbabwe [35], [36]. However it is seen as ineffective due to poor institutional arrangements, inadequate FiT level and hindrances in implementation [36]. A study by Huenteler highlighted one of the challenges for developing countries in implementing FiT to be the uncertainty in assigning roles to international donors and national governments, especially the role of balancing the FiT payments in markets with uncertain revenue streams [37]. Other country specific reasons exist as to why some developing counties have failed to implement successful FiT policies. For example, despite the efforts by Algeria to diversify its generation portfolio to include renewable and reduce reliance on fossil fuels, its FiT programme, first introduced in 2004, has not succeeded because of the strong reliance on fossil fuels that have a significant role in the economy [36], [38] By 2017 only 60 MWp combined installed capacity for PV and wind were achieved through the FiT programme since the start of its implementation [38]. In 2019 Kenya had only realized 0.66% of its target 1,551 MW that was planned to be achieved through its FiT policy that was first adopted in 2008 [39]. One of the reasons pointed out for this shortcoming was ineffective policy design, brought forth by lack of skills and competencies that were not readily available [39]

South Africa is particularly an interesting case. The country abandoned its FiT programme and adopted a tendering scheme in 2011 [36], [40]. As much as there was high interest from developers in the FiT programme, the problem was in its implementation. The National Energy Regulator of South Africa (NERSA) approved the renewable energy feed-in tariffs (ReFITs) in 2009, with tariffs set at 15.6 US cents/kWh for wind, 26 US cents/kWh for concentrated solar power and 49 US

cents/kWh for solar PV, prices which were seen as generous by developers [41]. This was after NERSA, through stakeholder and public consultations received comments on profitability of the projects through FiT, which was initially supported for 15 years [40]. There was however uncertainty remaining in the regulatory environment which caused delays in finalizing agreements, specifically power purchase and grid connection agreements with Eskom, the national utility. NERSA released a consultation paper in March 2011, with significant cuts in tariff prices to the shock of investors. The tariff cuts have been depicted in Table 2-1 [40]; Table 2-1: 2009 vs 2011 ReFIT Rates in South Africa

Technology	2009 ReFIT ZAR c/kWh			2011 ReFIT ZAR c/kWh	Percentage Change
Landfill Gas	125	93.8	-24.9		
Small Hydro	90			53.9	-40.1
CSP trough with storage	94			67.1	-28.6
CSP trough w/o storage	210			183.6	-12.6
CSP tower with storage	314			193.8	-38.8
Grid connected PV (≥ 1 MW)	231			139.9	-39.4
Biomass solid	394			231.1	-41.3
Biogas	118			106	-10.1
	96			83.7	-12.9

ReFIT was completely abandoned in South Africa in 2011 when the Department of Energy received advice that the programme was not in line with public finance and procurement laws [41]. Despite the failures seen in South Africa, FiT has been touted in most parts of the world as having had a positive impact in driving growth of renewable energy adoption [20], [25], [42]–[44].

Competitive auctioning or tendering, and quotas/renewable portfolio standards (RPS) are the two other prominent mechanisms besides FiT that are used to promote the adoption of renewable energy [25], [31]. Under a tendering scheme, the legislator reserves a certain quantity of installed capacity that is to be procured through a bidding process [19], [21], [25]. There are disadvantages however that are related to procuring renewable energy in this manner. Firstly, there is risk of loss to investors because the bid prices are usually set low to make the bid competitive. Secondly, long lead times from the bidding process to project completion, and finally operation, when investors can realize income render the projects not sustainably profitable [21]. The disadvantage of RPS is that the policy is restricting as it forces the utility companies and consumers to generate a specified portion of the electricity consumption from renewable sources [6], [43]. Because FiT guarantees access to the grid and periodic payments which ensures future income, and that it is not exposed to fluctuations in fossil fuel prices, it minimizes the risk of long term investment and improves the investment attractiveness of renewable energy sources [31]. FiT has driven growth of renewable energy technologies through new installations, realizing 87% of global PV capacity by 2014 [37]. This if further supported by a comparative study between FiT and RPS by Sun and Nie which concluded that FiT is more efficient in increasing the deployment of renewable energy sources [43].

2.2.Tariff Design Options

Tariff design options define the basic rules that govern how electricity producers can sell electricity to the off-taker, while also seeking to establish a comprehensive FiT scheme [19]. Most of the studied sources of literature on tariff design option list different basic tariff design options, however this paper will discuss eligibility, tariff duration, inflation indexation, tariff degression, size-specific tariffs, tariff calculation methodology, purchase obligation as well as locationspecific tariff. These options are chosen because they are basic and would not bring complexities for a country that has not had a FiT policy before. Tariff design options are important because they have an influence on the tariff price.

2.2.1. Eligibility

Eligibility of the renewable power plants to be included under the FiT scheme is commonly determined by technology type and installed plant size. Policy makers choose the types of renewable energy technologies that can be included under the FiT scheme mainly influenced by availability of the resource under question [21]. Plant size or installed capacity is also commonly used to define eligibility by giving the minimum and maximum plant capacities that will be eligible for FiT scheme

[22]. Germany's EEG lists many technologies including solar PV, solar thermal, hydro tidal and wind as eligible technologies [19]. In Spain, the legislation includes technologies with precise definitions in solar, wind, waste, hydro, geothermal and wave energy [19]

2.2.2. Duration

It is important for the FiT scheme to state the duration of support during which FiT payments will be made to investors. Long FiT periods are desirable because they facilitate good financing conditions with low interest rates, resulting in lower levelized payments [19]. Typically, FiT support duration ranges from 20 to 25 years, which is usually based on the expected life span of many installations [21]. However there still exist shorter support periods ranging from 15 to 20 years. Schemes with long time periods, 20-25 years are usually encouraged to consider the impact of inflation when determining the level of payment [21]. Since the start of its implementation, Germany's EEG guaranteed a support duration of 20 years for all renewable sources. Support duration in France varies between 15 and 20 years across different renewable energy technologies. In South Africa the FiT scheme guaranteed support for all renewables for a period of 20 years [19], [21].

2.2.3. Inflation Indexation

Adjusting the FiT to inflation, also known as inflation indexation means the FiT payment is adjusted up partially or fully according to the annual inflation where the scheme is being applied. Inflation indexation is included in the FiT scheme in order to protect the real value of a renewable energy investment from exposure to economic activities over its economic lifetime [22]. According to Mendoca et al., inflation indexation is particularly necessary in countries with high level of inflation as the real value of the investment in a long term scheme will be significantly lower than the initial value if indexation is not applied [21]. Some of the countries that practise inflation indexation are Ireland, Canada and Spain [21]. In Ireland, the legislator fully adjusts FiT payments to the annual inflation rate. In Canadian province of Ontario, the legislator adjusts only 20% of the tariff payments to the annual inflation [45].

2.2.4. Tariff Degression

Tariff degression means the tariff levels for new plants are reduced by a certain percentage each year after the start of FiT scheme implementation [23]. Tariff degression affects only new installations. Once a plant is installed, the tariff that applies to it is not affected by this option [21]. Policymakers

apply tariff degression because they anticipate technological advances, economies of scale and learning process [19], [23]. The learning process is the relationship between technology costs and overall industrial output in which when doubling cumulative output, the total costs decrease by a certain percentage known as learning rates [23]. Tariff degression affects technological advances in that when tariff is reduced each year, manufacturing sector is forced to continually improve on their products in order to pass the reductions to the buyers of the technology [19].

2.2.5. Size Specific Tariff

Policymakers have the choice to set different tariff payments based on the plant size. This is mainly because of the significantly different installed costs for different plant capacities [46]. For solar PV, the common practice is to differentiate plant sizes by typical installed capacities to represent domestic rooftop, commercial rooftop and utility ground mount installations [21].

2.2.6. Tariff Calculation Methodology

Tariff setting methodologies generally follow two main approaches, which are cost-based approach and value-based approach [19]. Value-based approach takes the value of the firm in terms of the avoided costs of power generation, if the same amount of electricity was being generated from a conventional plant, as the benchmark for tariff setting [19], [22]. Cost-based approach takes the technology specific costs of generation - investment costs and operational costs - as the benchmark for tariff setting [19]. In the cost-based approach policymakers usually apply a reasonable return on investment as a profitability margin [21]. The cost-based approach has been reported as historically more efficient and effective for renewables than the value-based approach [22]. In setting FiT for renewable sources, Germany uses the cost-covering remuneration in which the tariffs are set to allow investors to fully recover the costs of generation [19]. The methodology assumes interest on capital at a rate of 8% per annum, annual inflation of 2%. An annuity method is then applied to produce periodic payments from the determined once-off payment [21]. In France, a profitability index method is applied in determining the FiT [21]. The profitability index is defined as the ratio between the net present value of an investment and its investment costs. The legislator in France applies the weighted average cost of capital (WACC) as the discount rate, as opposed to the targeted IRR, a depreciation period of 15 years is assumed [19], [21]. South Africa's NERSA uses a levelized cost of electricity approach. This approach aims for full cost recovery plus a reasonable return on invested

capital [21]. NERSA makes the following economic assumptions for calculating the FiT; debt to equity ratio of 70:30, inflation of 8%, tax rate of 29% and real WACC of 12% [47].

2.2.7. Purchase Obligation

A purchase obligation forces the offtaker to purchase all electricity that is produced by the renewable power plant regardless of the demand of electricity. This feature increases investment security by ensuring that all electricity will be purchased from the power plant immediately after its start of operation [19]. A purchase obligation is particularly important for non-dispatchable renewable energy sources like wind and solar where the amount of electricity produced cannot be controlled to match the demand [21].

2.2.8. Location Specific Tariff

In order to avoid unreasonably high profits for producers at high quality resource sites and to assist producers at low quality resource sites to achieve profitability, policymakers have the option to set tariffs for different locations based on the quality of the renewable resource. This means sites with high quality resource receive lower FiT payments than sites with low quality resource [19]. Since 2000, Germany has been using location specific FiT scheme for its wind industry, while France started implementing location specific FiT scheme for wind in 2001 and for solar PV in 2010 [19].

2.3.Review of Solar PV Costs

The cost of solar PV plants has fallen significantly in the past decade driven mostly by falling solar module prices. A 2019 analysis by IRENA showed that the prices of solar modules have fallen by more than 90% between 2009 and 2018, which has been a major influencing factor in the global weighted average installed cost of solar PV plants, falling from USD 4,621 to USD 1,210 in the same period [7]. Figure 2-2 shows the global weighted average installed costs of solar PV plants together with the 5^{th} and 95^{th} percentiles from 2010 to 2018.

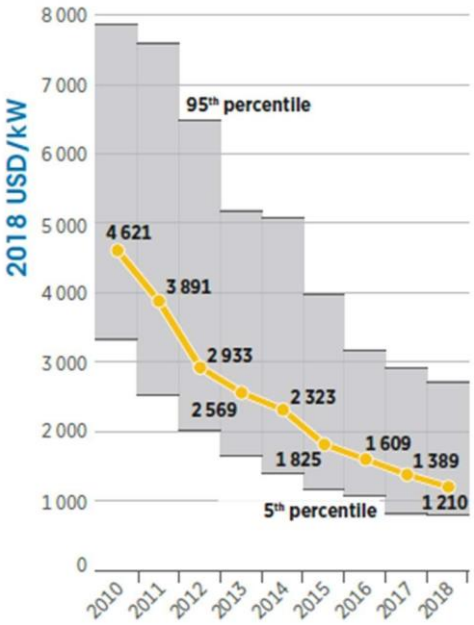

Figure 2-2: Global Weighted Average Installed Costs for Solar PV Source [7]

In terms of LCOE, the global weighted average LCOE for utility scale solar PV plants fell from USD 0.37 in 2010 to USD 0.09 in 2018, with prices in China and India being lower than the average at USD 0.067 and USD 0.063 respectively[7]. Figure 2-3 shows the global weighted average LCOE together with 5th and 95th percentiles.

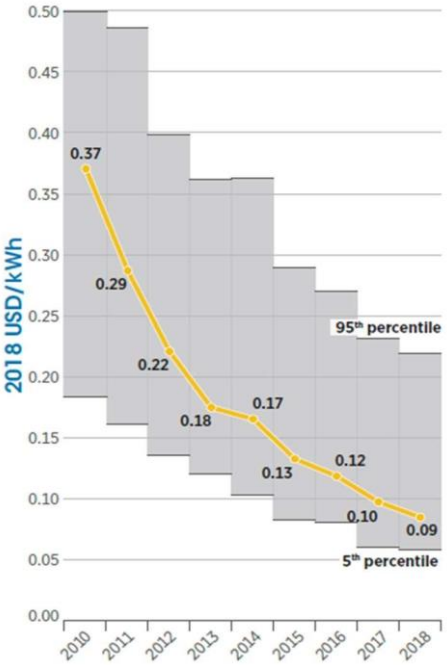

Figure 2-3: Global Weighted Average LCOE Source [7]

The National Renewable Energy Laboratory (NREL) tracks and benchmarks the solar PV costs for residential, commercial and utility-scale systems in the United States. A report for the first quarter of 2018 showed that the installed cost of utility scale fixed tilt solar PV plants was as low as USD 1.06/Wdc [48]. The results of the report on installed solar PV costs have been summarized in Table 2-2.

Table 2-2: Installed Costs for Q1 2018 in the US Source [48]

System Type	Description	Size	Installed Cost
Residential	Rooftop systems for residential sector	3 - 10 kW	USD 2.70/Wdc USD 3.11/Wac
Commercial	Rooftop systems installed in commercial centers	10 – 2,000 kW	USD 1.83/Wdc USD 2.10/Wac
Utility Scale	Ground mounted utility scale systems (Fixed tilt)	>2,000 kW	USD 1.06/Wdc USD 1.44/Wac

The report further showed a sharp fall in installed costs for solar PV plants from 2010 to 2018. In the residential sector, installed costs fell from USD 7.34/Wdc to USD 2.70/Wdc, USD 5.43/Wdc to USD 1.83/Wdc in the commercial sector, while the prices for fixed tilt utility systems fell from USD 4.63/Wdc to USD 1.06/Wdc [48]. Figure 2-4 shows the comparison in installed costs from 2010 to 2018 for different sectors;

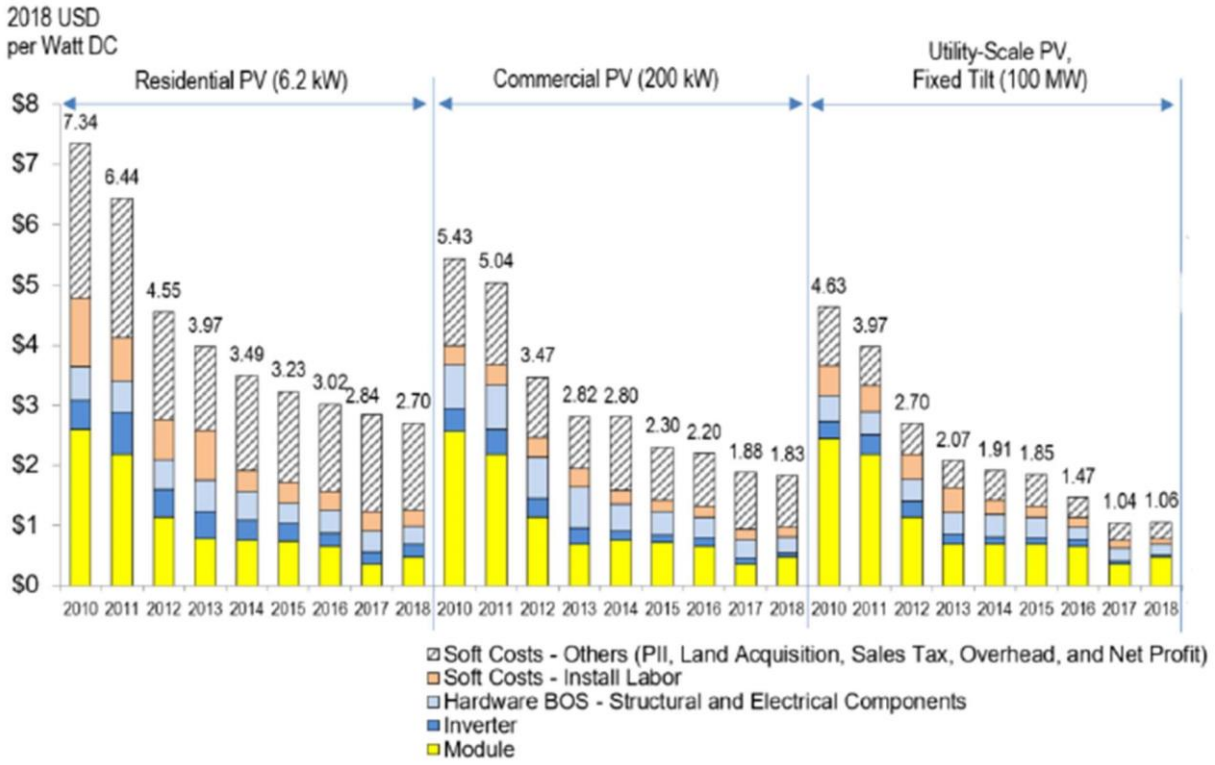

Figure 2-4: Installed Costs for solar PV Systems from 2010 to 2018 in the US Source [48]

The falling installed costs of solar PV plants are mainly attributed to increased solar module efficiencies, and lower inverter prices among others [48]. The falling installed costs of solar PV systems have also influenced the LCOE, which has also been on a downward trend from 2010 to 2018 as show in Table 2-3;

Table 2-3: 2010 & 2018 LCOE ranges for Solar PV systems in the US Source [48]

System Type	2010 LCOE (USD/kWh)	2018 LCOE (USD/kWh)
Residential	0.42 – 0.55	0.12 – 0.16
Commercial	0.32 – 0.41	0.09 – 0.12
Utility Scale	0.24 – 0.28	0.04 – 0.06

Operating and maintenance (O&M) costs are an important factor to consider because of their impact on the life cycle cost of solar PV plants. The O&M costs include costs incurred for scheduled

preventative maintenance as well as corrective costs incurred for replacement of components [49]. Data from the International Energy Agency (IEA) World Energy Outlook 2016 showed that among other varying parameters that feed into the FiT, namely capital costs, capacity factor, WACC and the economic lifetime, the O&M costs can cause the base FiT price to change by between -5% and +5% meaning the FiT is sensitive to change in the O&M costs. Figure 2-5 the sensitivity of LCOE to several input parameters, including O&M costs [50]

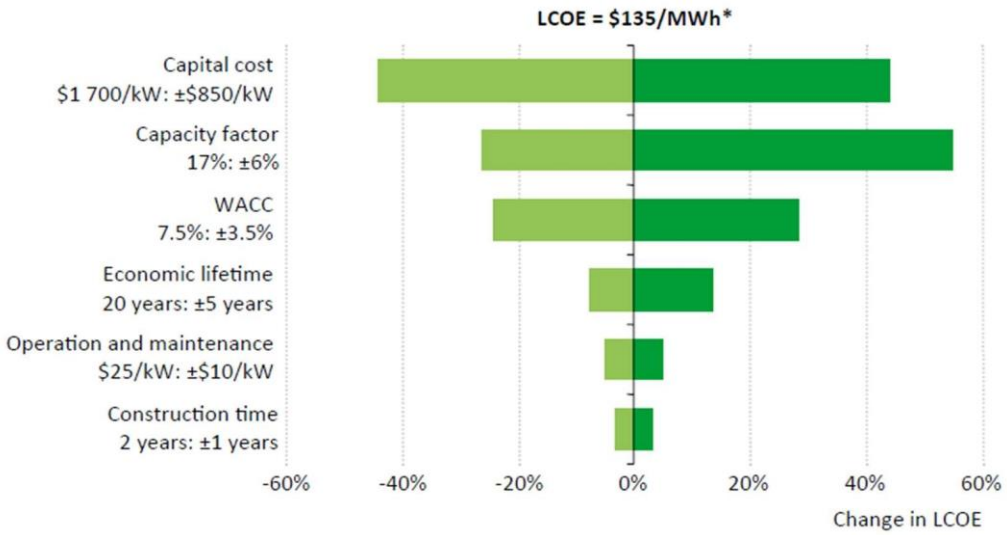

Figure 2-5: Sensitivity of LCOE to Input Parameters Source [50]

The NREL benchmark study for solar PV costs for the first quarter of 2018 shows that O&M costs varied on an annual basis from USD 9.10/kW to USD 12.00/kW for different system types [48]. Figure 2- 6 shows the O&M costs for residential, commercial and utility scale systems;

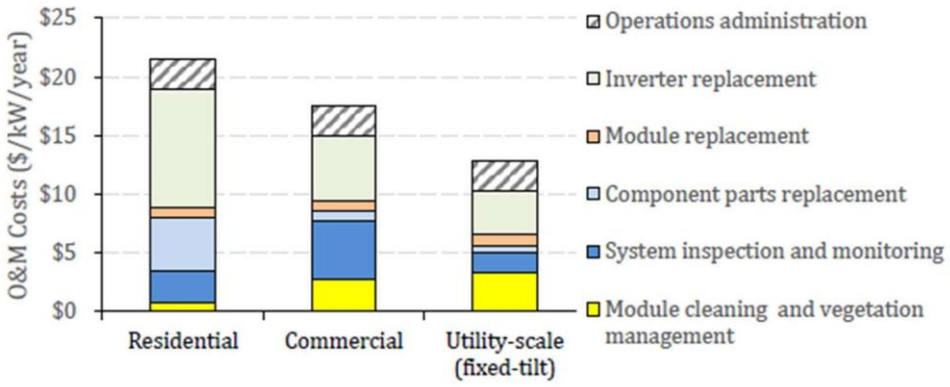

Figure 2-6: O&M Costs for Residential, Commercial and Utility Scale PV Systems Source [49]

2.4. Radiation Received on a Tilted Collector

The sun continuously emits radiant energy in all directions at the rate of 3.845 × 10 W, out of which the earth receives 1.7 × 10 W [51]. In terms of power density or irradiance, the earth receives 1367 W/m outside its atmosphere, a figure known as the solar constant, denoted G_{sc} [52]. Before reaching the surface of the earth, some of this radiation is absorbed, some is scattered while some is reflected [52]. The surface of the earth then receives radiation in two major components. The first component is called beam radiation I_b, which is the direct radiation received without being absorbed or scattered. The second component is the diffuse radiation I_d, which is the radiation received on the surface of the earth after being scattered in the atmosphere. The sum of beam and diffuse components is known as the global radiation, commonly measured as total radiation received on a horizontal surface, termed global horizontal radiation [53]. The angle of incidence is important to consider because it is used to determine the beam radiation that is incident on a flat surface with an arbitrary tilt. The relationship between angle of incidence θ, and beam radiation incident on a tilted surface is given by [54];

$$ = \cos \qquad 2.1$$

Where is the beam radiation on a flat surface perpendicular to the incident radiation.

2.4.1. Angle of Incidence, θ

The geometric relationship between a flat surface on earth and incident solar radiation is important because it determines at any instant how much of the global radiation is collected by the surface. A set of angles describing this relationship are as follows, based on references [51], [53];

Latitude, φ: Latitude is the angular location from the equatorial plane to the location of the collector, north or south of the equator. Locations in the north of equator have positive latitude and south of the equator have negative latitude values.

Declination angle, δ: Declination angle is the angular distance from the sun rays at solar noon, and the equatorial plane. The declination angle ranges from 0° to 23.45° in the northern hemisphere and 0° to -23.45° in the southern hemisphere. The declination angle is calculated using Equation 2.2

$$ = 23.45\sin \frac{360}{365}(284 +) \qquad 2.2$$

where N is the day number in year.

Slope/Tilt, β: Slope or tilt is the angle between the surface and the horizontal. Tilt angle of 0° means the surface is horizontal, while tilt angle of 90° means the surface is vertical.

Surface Azimuth, γ: This is the angle between the horizontal projection of the normal to the surface, and true south, with south = 0°, and westward angles positive.

Hour angle, ω: Hour angle is the angle between the local meridian and the position of the sun, measured east or west of the meridian. The hour angle is negative in the morning and positive in the afternoon.

Using the above definitions, the angle of incidence is defined as the angle between the normal to a surface and the beam radiation incident to that surface [53]. Equation 2.3 expresses the angle of incidence in terms of latitude declination, surface tilt, surface azimuth and hour angle [55];

□ = □□□ (□□□□□□□□□□□□ − □□□□□□□□□□□□□□□□ + □□□□□□□□□□□□□□□□ 2.3

+ □□□□□□□□□□□□□□□□□□□□ + □□□□□□□□□□□□□□□□)

Figure 2-7 shows the schematic representation of latitude φ, declination angle δ, surface tilt β, surface azimuth γ, hour angle ω and the angle of incidence θ;

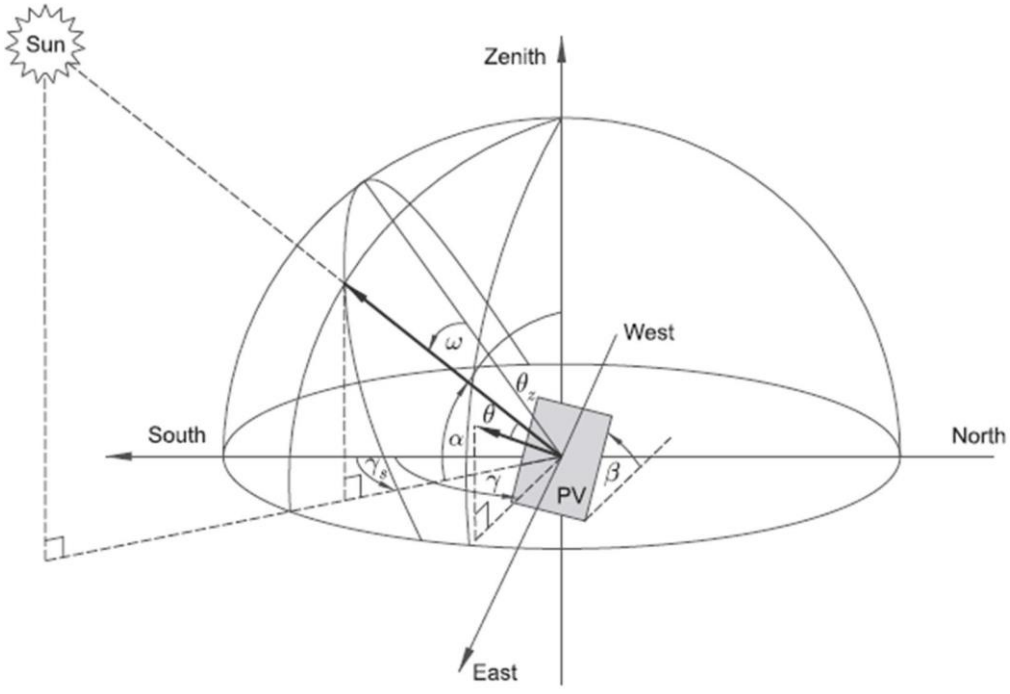

Figure 2-7: Representation of Solar Geometric Angles; Source [56]

For a horizontal surface, the angle of incidence becomes the zenith angle θ_z and is expressed by Equation 2.4 [54];

$$\cos \square = \sin \square \sin \square + \cos \square \cos \square \cos \square \quad 2.4$$

2.4.2. Hourly Radiation on a Tilted Collector, I_T

Most measured radiation data is available as global radiation and diffuse radiation on a horizontal surface [57]. However for analysis of short and long term performance of solar collectors and photovoltaics, radiation on tilted surfaces is required [58]–[60]. Hence why models have been developed to estimate radiation on tilted surfaces from that on horizontal surfaces [57]. There are two main classes of such models, namely isotropic models and anisotropic models [58]. The two classes differ in how they treat the three parts of diffuse radiation incident on a tilted collector, which are isotropic, circumsolar and horizon brightening parts [53]. Isotropic models assume that diffuse radiation is spread uniformly across the sky dome [57], while for anisotropic models, above the diffuse radiation on the sky dome, they also consider diffuse radiation on the solar disk, that is the circular region where the sun is positioned [53], [58]. The two classes are derived from the equation that expresses the total radiation on a tilted surface as a sum of beam radiation, diffuse radiation and reflected radiation as [57], [61];

$$\square = \square_{,} + \square_{,} + \square_{,} \quad 2.5$$

Where,

- $\square_{,}$ is the hourly beam radiation on a tilted surface
- $\square_{,}$ is the hourly diffuse radiation on a tilted surface
- $\square_{,}$ is the hourly reflected radiation on a tilted surface

Some of the reviewed isotropic and anisotropic models have been presented in the following sections;

Liu and Jordan: In 1963 Liu and Jordan developed an isotropic model that assumed both diffuse and ground-reflected radiation are isotropic [53]. According to this model the total radiation on a tilted surface is therefore given by Equation 2.6 [53], [57];

$$\square = \square\ \square + \square\ \frac{1 + \cos \square}{2} + \square\square\ \frac{1 - \cos \square}{2} \quad 2.6$$

Where;

$\square$ is the beam radiation on a horizontal surface

$\square$ is the diffuse radiation on a horizontal surface

$\square$ is the total radiation on a horizontal surface

$\square$ is the slope or tilt of a surface

$\square$ is the ground albedo

$\square$ is the ratio of beam radiation on a tilted surface to that on a horizontal surface given by Equation 2.7 [62];

$$\square = \frac{\square_{,}}{\square} = \frac{\cos \square}{\cos \square} \quad 2.7$$

Where $\square$ is the zenith angle.
The three components of total radiation, which are beam radiation $\square_{,}$, diffuse radiation $\square_{,}$ and reflected radiation $\square_{,}$ from Equation 2.5 are represented by the Liu and Jordan model in Equation 2.6 as follows [53];

$$\square_{,} = \square\ \square \quad 2.8$$

$$\square_{,} = \square\ \frac{1 + \cos \square}{2} \quad 2.9$$

$$\square_{,} = \square\square\ \frac{1 - \cos \square}{2} \quad 2.10$$

Hay and Davis: Hay and Davis developed an anisotropic model in 1980 by assuming the diffuse radiation is made up of isotropic and circumsolar components [58]. This model estimates the fraction of radiation that comes from the circumsolar components but does not consider the horizon brightening component. According to this model, the total radiation on a tilted surface is given by [53];

$$\square = (\square + \square\,\square)\square \quad \frac{1}{2} + \square\,(1 - \square)\,\frac{1 + \cos\square}{2} + \square\square\,\frac{1 - \cos\square}{2} \qquad 2.11$$

Where $\square$ is the anisotropy index. The rest of the terms retain the meaning as in Equation 2.6.

HDKR model: In 1990 Reindl improved the Hay and Davies model by adding a term that estimates radiation as a result of horizon brightening, as proposed by Klutcher [53]. The resulting model for total radiation on a tilted collector is thus given by Equation 2.12;

$$\square = (\square + \square\,\square)\square + \square\,(1 - \square)\,\frac{1 + \cos\square}{2}\,\frac{1 + \square\sin\frac{\square}{2}}{} + \square\square\,\frac{1 - \cos\square}{2} \qquad 2.12$$

Where f is a modulating factor that accounts for cloudiness [53]. The rest of the terms retain the meaning as in Equation 2.6.

Perez model: The Perez model is an anisotropic radiation model and it conducts a detailed analysis of all three components of the diffuse radiation [60]. The resulting model is given by Equation 2.13;

$$\square = \square\,\square + \square\,(1 - \square)\,\frac{1 + \cos\square}{2}\Big) + \square\,\square\,\frac{\square}{\square} + \square\,\square\sin\square + \square\square\,\frac{1 - \cos\square}{2} \qquad 2.13$$

where $\square$ is the circumsolar coefficient and $\square$ is the horizon brightening coefficient [60]. The terms a and b are calculated as;

$$\square = \max(0, \cos\square),\ \square = \max(\cos 85°, \cos\square) \qquad 2.14$$

$\square$ and $\square$ are functions of zenith angle $\square$, brightness coefficient Δ and clearness $\square$, all three which describe the sky condition[53]. The clearness $\square$ is given by;

$$\square = \frac{\frac{\square + \square_{,}}{I_d} + 5.535 \times 10^{-6}\theta_z^3}{1 + 5.535 \times 10\ \square} \qquad 2.15$$

where $\square_{,}$ is the normal beam radiation and $\square$ .is in degrees.

Brightness coefficient Δ is given by;

$$\Delta = \frac{m \cdot E_{dn}}{E_0} \quad 2.16$$

where m is the air mass and E_0 is the extraterrestrial normal incidence radiation [53]. ε and Δ can be estimated using Equations 2.17 and 2.18 [53];

$$\theta_z = \max\left(0, \cos^{-1}\left(\sin\beta + \Delta + \frac{1.6}{180}\right)\right) \quad 2.17$$

$$\varepsilon = \frac{\theta_z^2 + \beta + \frac{1.6}{180}}{\theta_z^2 + 5.3 + \frac{1.6}{180}} \quad 2.18$$

The irradiance coefficients F_{11}, F_{12}, F_{13}, F_{21}, F_{22} and F_{23} used in Equations 2.17 and 2.18 have been presented in Table 2-4;

Table 2-4: Irradiance coefficients for Perez Model Source [53]

Range of ε	F_{11}	F_{12}	F_{13}	F_{21}	F_{22}	F_{23}
1.000-1.065	-0.062	-0.060	0.072	-0.022		
1.065-1.230	-0.151	-0.019	0.066	-0.029		
1.230-1.500	-0.221	0.055	-0.064	-0.026		
1.500-1.950	-0.295	0.109	-0.152	0.014		
1.950-2.800	-0.362	0.226	-0.462	0.001		
2.800-4.500	-0.412	0.288	-0.823	0.056		
4.500-6.200	-0.359	0.264	-1.127	0.131		
6.200-	-0.250	0.156	-1.377	0.251		

In their study that compared models for global tilted radiation, Danandeh and Mousavi, the authors of reference [55] concluded that models work differently for different latitudes and therefore there is no single model that is suitable for all countries. The reviewed studies that compare tilted radiation

models draw different conclusions, however different experimental setups are also observed. For example authors of reference [60] compared five models with measured global tilted and global horizontal radiation data in Hannover, Germany and Colorado, USA. The study concluded that the Perez model provides the best estimates of global tilted radiation for surfaces facing south. Authors of reference [58] compared three isotropic models to three anisotropic models, and evaluated the two classes with measured data in Bhopal, India. The study compared Liu and Jordan, Koronakis, Badescu, Hay and Davies, Reindl et al. and HDKR models at a fixed angle of 23.26° facing south. The study concluded that the Hay and Davies model gave the highest estimate of all models, and that the preferred model was the Badescu model. Another study that compared the tilted radiation models is in reference [62]. The authors compared Hottel and Woertz, Hay and Davies two models by Perez and a model by Hay, Davis, Temps and Coulson. The authors used data from Albany, New York and San Antonio Texas to compare the results of each model for hourly tilted radiation with the measured data. The study concluded that all anisotropic models had the best and similar performance, with the Perez model being the best performing model. All these studies have generally agreed that the isotropic models under-predicts tilted radiation, while the anisotropic models, particularly the Perez model over-predicts tilted radiation [60], [62].

In Lesotho two models have been used in two studies. The author in reference [63] used the Liu and Jordan model to determine radiation incident on surfaces with different orientation and slopes in three places in Lesotho, while the authors in reference [59] determined the monthly global tilted radiation on surfaces facing the equator at different inclinations at Maseru, Lusaka and Harare. The tilted radiation model used for the second study was the anisotropic Hay model. The authors in reference [59] further suggested that both Hay model and Liu and Jordan models are equally suitable for estimation of tilted radiation in Lesotho and in generally in Southern Africa, both resulting in mean percentage error of within 3%.

The tilt angle of the flat solar collector with respect to the horizontal is an important determining factor of solar energy output for a given period [56]. Optimizing a tilt angle is determining an angle that will give the maximum array yield for a specified period [64]. There are many studies determining the optimum tilt angle for different locations. The authors in reference [56] determine the optimal tilt angle in Belgrade for different study periods; daily, fortnightly, monthly and annually. Danandeh and Mousavi determine the optimum tilt angle for different cities in Iran using different global tilted radiation models [55]. In Lesotho a study was carried out to determine the

monthly average daily radiation on surfaces with different orientations for tilt angle equal to □ + 15°, □, and □ − 15°, where φ is the angle of latitude. The study was carried out for two locations, namely Oxbow and Ts'akholo [63]. The author made the following conclusions;

- That the optimum tilt angle for all orientations for November, December and January is □ − 15°.
- That for May, June July, the optimum tilt angle is □ + 15° for azimuth less than 130°, and □ − 15° for higher azimuths.
- That for azimuth less than 150° the optimum tilt angle for maximum annual yield is equal to the latitude itself.

2.5.Solar Energy Output

A solar module converts some of the incident radiation on its surface to electricity, typically with 6-20% efficiency [65]. Typically, solar modules are evaluated for performance using controlled environmental conditions. The IEC 61853-1, Standard Test Conditions (STC) evaluates solar modules under incident irradiance of 1000 W/m^2, cell temperature of 25°C, air mass of AM 1.5 and wind speed of zero [66]. However these conditions are rarely ever met under field operation [66]. Several factors affect the field performance of solar modules. These factors are cell temperature, losses due to soiling, shading and other capture losses as well degradation. These factors are discussed in the following subsections.

2.5.1. Cell Temperature

Increasing cell temperature reduces the power output and efficiency of solar modules [67]. This reduction in performance is caused by high carrier concentration, which results in high number of recombination [65]. There are generally two groups of models correlating ambient temperature to the performance of solar PV modules. One group correlates the cell operating temperature T_c to the environmental variables, such as wind speed WS, ambient temperature T_a, irradiance $I_{T,}$ as well as solar module material properties. The other group correlates the dependence of solar PV Standard Test Conditions (STC) efficiency η_{STC} to cell operating temperature T_c.[65]. Dubey et al. reviewed different correlation models for solar module efficiency and ambient temperature and notes that most models reveal a linear relationship between module power output and cell temperature. The study further reveals that most models reduce to the expression depicted by Equation 2.19 [65]

$$\square = \square \quad [1 - \square(\square - \square \quad)] \qquad 2.19$$

Where;

$\square$ is the cell field efficiency

$\square$ is the efficiency under STC

$\square$ is the module temperature coefficient

$\square$ is the cell operating temperature

$\square$ is the STC temperature

The Sandia National Laboratories model presented in Equation 2.20 determines the average temperature of a module given the environmental parameters and empirically determined coefficients [68];

$$\square = \square \cdot (\square \quad \cdot \quad) + \square \qquad 2.20$$

Where;

$\square$ is the average temperature of the back surface of the module

$\square$ is the solar irradiance incident on the solar module

$\square$ is the ambient temperature WS

is the wind speed

a is the coefficient that imposes upper limit for temperature of the module at low wind speed and high irradiance

b is the coefficient that establishes the rate for drop in module temperature with increasing wind speed.

2.5.2. Losses

Capture losses can be caused by presence of snow on the solar array, cell temperature that is above 25°C, dust or partial shading[69] [70]. Several studies have reported annual losses due to show as high as 3.5% in Japan, 2.7% in Germany and 3.3% in Austria [70]. Another cause of capture losses is soiling [71]. Soiling is the presence of contaminants on the surface of solar modules, like bird droppings, plant debris, industrial fumes and dust [72]. The impacts of soiling depends on the tilt angle, with modules tilted at less than 30° being most affected [70]. Figure 2 - 8 shows the annual

losses in different countries due to soiling. Other reported causes of capture losses are shading, lack of maximum power point tracking (MPPT) device and high module temperature [52].

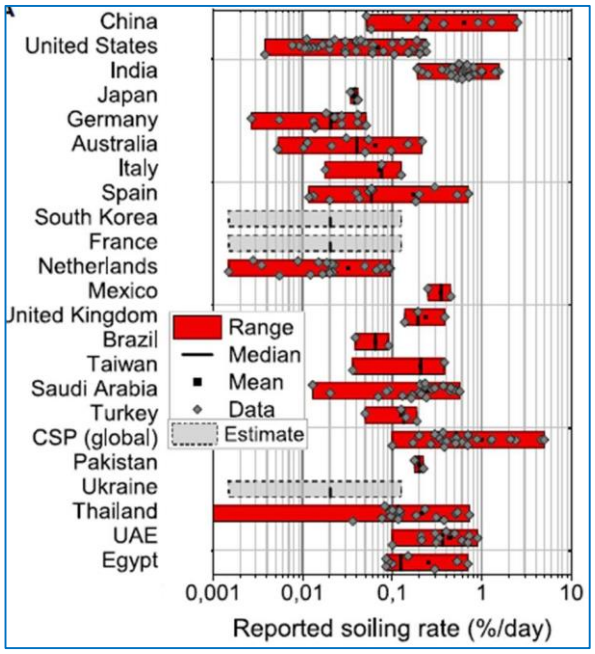

Figure 2-8: Global impact of soiling Source [72]

2.5.3. Annual Degradation:

Degradation is another important factor that affects the field performance of solar modules. Degradation of solar modules over time is the reduction in power output over time [73]. Solar modules are subject to degradation typically a rapid decline in the first year of operation, and a gradual long term degradation thereafter [70]. Hot and humid regions are reported as having the highest degradation rates [74]. Many studies have reported different annual degradation rates for many solar cell technologies. In their performance analysis of a 99.84 kWp grid connected system in its first six years of operation, Roumpakias and Stamatelos report an annual degradation rate between 1% and 4% [75]. Limmanee et al. found that after four years of operation, solar modules made from thin film silicon had an annual degradation rate of up to 6.1%, while other types of modules, including crystalline silicon, had an annual degradation rate ranging from 1.2% to 1.8% [74]. In their study of more than 2000 degradation rates reported in literature, Jordan and Kurtz

found an average degradation rate of 0.8% per annum, with the median value of 0.5% [73]. Figure 2-9 shows a histogram constructed from the reported annual degradation rates for all photovoltaic technologies, including thin film and crystalline silicon.

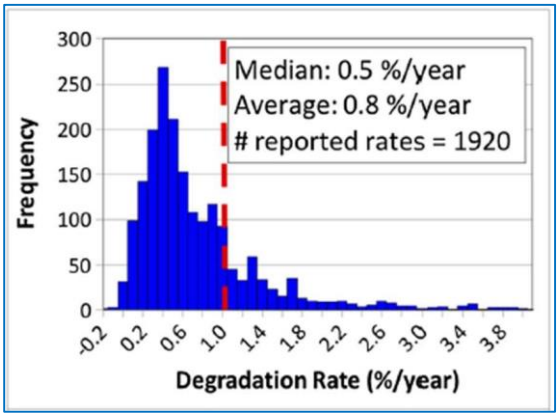

Figure 2-9: Histogram of Annual Degradation Rates Source [73]

Consequently the power output of solar modules is given by Equation 2.21 [76];

$$\square\ \square\ \square = \frac{\square}{\square} \cdot \square \cdot \square \qquad 2.21$$

Where;

$\square$ is the power output of solar modules

$\square$ is the field efficiency of the solar modules

$\square$ is the rated efficiency of the solar modules

$\square$ is the total irradiance on a tilted collector

$\square$ is the reference irradiance (1000 $\square/\square$) $\square$ is the rated power of the solar array

The power at the output of the inverter $\square$ can then be determined by solar power output $\square$, inverter efficiency $\square$ and the efficiency of wiring as $\square$ [77];

$$\square = \square \cdot \square \cdot \square \qquad 2.22$$

2.6. Performance Indices

The IEC standard 61724 states normalized performance indicators or indices that can be used to compare different solar PV systems [5], [74]. These performance indices are reference yield Y_R, array yield Y_A, final yield Y_F, performance ratio PR, collection losses L_C and system losses L_S [52]. These indices account for the performance of a system taking into account the energy production, solar energy resource and losses for the period of analysis [78]. Figure 2-10 shows a graphical depiction of the performance indices.

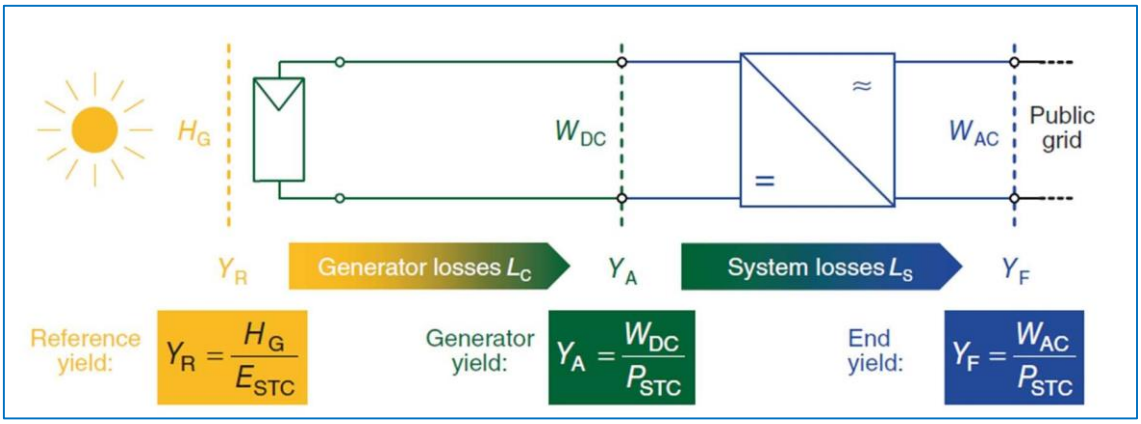

Figure 2-10: A Figure of Reference, Array and Final Yields, Source [52]

The performance indices are defined as follows;

2.6.1. Reference Yield, Y_R

The reference yield is the total in-plane radiation H_T divided by the irradiance under Standard Test Conditions (STC) conditions of 1000 W/m^2. It gives the number of hours within the observed period that the sun would have been emitting irradiance at 1000 W/m^2 [71]. The equation for reference yield is given as [78];

$$\square = \frac{\square}{\square} \qquad 2.23$$

Where $\square$ is the reference yield, $\square$ is the total in-plane radiation and $\square$ is the irradiance at STC.

2.6.2. Array Yield, Y_A

Array yield is the actual energy output from the array E_{DC} divided by the array rated power P_{STC}. The array shows the actual energy production for each installed unit power of the array over an observed period [52]. The equation for array yield is [78];

$$\square = \frac{\square}{\square} \qquad 2.24$$

2.6.3. Final Yield, Y_F

The energy out of the inverter into the grid E_{AC} divided by the array rated power P_{STC} gives the final yield Y_F for an observed period [71]. The equation for final yield is given as [78];

$$\square = \frac{\square}{\square} \qquad 2.25$$

2.6.4. Performance Ratio, PR

The performance ratio is a measure of how much of the reference radiation the system can convert to energy injected into the grid [52]. It is a dimensionless quantity of how much losses occur in the system due to inverter operation, tripping circuit breakers and other system failures [71]. The equation for performance ratio is given as [78];

$$\square\square = \frac{\square}{\square} \qquad 2.26$$

2.6.5. Collection Losses, L_C

Collection losses occur in a solar PV system due to inefficient operation of the PV array. Causes of collection losses are modules operating at cell temperature above 25°C, modules being soiled or shaded, mismatch in current or voltage among the strings and ohmic losses [52], [71]. The equation for collection losses is given as [78];

$$\square = \square - \square \qquad 2.27$$

Where Y_R and Y_A are reference and array yield respectively.

2.6.6. System Losses, L_S

System losses occur during the conversion of array DC energy to AC energy [71]. The main caused of system losses are inverter efficiency which is less than 100%, cable losses and under-sized inverter that does not match DC power output [52]. The equation for system losses is given as [78];

$$\square = \square - \square \qquad 2.28$$

Where Y_F and Y_A are final and array yields respectively.

2.7. Bilinear Interpolation

Bilinear interpolation is a technique popular in geographical information systems (GIS) and image processing [79], [80]. In GIS it is used to estimate the value of a point in a two dimensional grid, based on the values of its four closest neighbors, and using their weight determined by the distance from the point of interest [79], [81]. Figure 2-11 shows bilinear interpolation in a grid of two dimensions on the x-axis and y-axis;

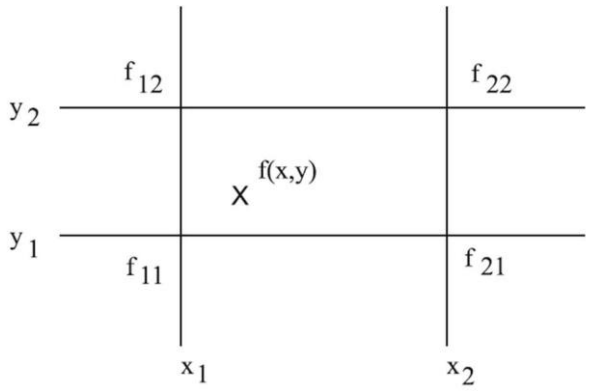

Figure 2-11: Bilinear interpolation in and (x,y) grid Source [80]

From Figure 2-11, bilinear interpolation can be used to estimate the value of point X at an arbitrary location (□, □) using the values of the points at discrete locations (□ , □), (□ , □), (□ , □) and (□ , □) with values □ , □ , □ and □ respectively, by solving a system of linear equations as presented Equation 2.29 [80];

$$\begin{aligned} f_{11} &= a + bx_1 + cy_1 + dx_1y_1 \\ f_{12} &= a + bx_1 + cy_2 + dx_1y_2 \\ f_{22} &= a + bx_2 + cy_2 + dx_2y_2 \\ f_{21} &= a + bx_2 + cy_1 + dx_2y_1 \end{aligned} \qquad 2.29$$

a, b, c, and d are coefficients. Using the coefficients given by Equations 2.30 to 2.33;

□ = □ − □□ − □□ − □□ □ 2.30

□ − □
□ − □□) 2.31
□ − □

□ − □
□ =) 2.32
□ − □

□ − □ − □ + □
□ = 2.33
(□ − □)(□ − □)

When the coefficients have been determined, the value of X can then be determine by Equation 2.34 [80];

□(□□) = □ + □□ + □□ + □□ 2.34

3. MATERIALS AND METHODS

3.1. Data Used

In order to determine the FiT for Lesotho and assess the necessity for setting different tariffs for different locations, the Typical Meteorological Year (TMY) data was used from European Commission Photovoltaic Geographical Information System (PVGIS) in reference [82]. TMY data was first developed by Sandia National Laboratory by choosing meteorological data for twelve months that are representative of the long term data available in the database [83]. Other studies that have used TMY data include a study by Martin and Ruiz to calculate angular losses of PV modules in 10 site in Europe [84] This data was chosen because it is free and can be downloaded all points in 0.25° latitudinal and longitudinal grid. It is available in hourly time, which is suitable for the analysis of this study.

3.2. Gridding

Since one of the objectives of the study is to determine the necessity to set a different feed-in tariff for different locations in Lesotho, it therefore becomes necessary to know the annual array yield □ at any given location within Lesotho. The procedure taken in order to achieve this was to divide the area covering Lesotho from 27° to 30° East, and 28° to 31° South into grid points spaced at 0.25° on both the longitude and the latitude. This resulted in 169 grid points, at which to determine the

annual array yield. The grid points, with their (x,y) values representing their coordinates were then added to Surfer software together with their respective z values representing the array yield □ to produce a contour map than can then be used for dividing the country into different regions. A more comprehensive discussion on this exercise of zoning can be found in the succeeding Section 3.6.

3.3. Determination of Incident Radiation

3.3.1. Equations and Models

The necessity to determine radiation on tilted flat surface from global horizontal radiation was discussed in Section 2.4.2. Isotropic and anisotropic models used for this purpose were also discussed. To determine the hourly incident radiation on tilted surface I_T, Liu and Jordan model as depicted by Equation 2.6 was used. This model was chosen mainly for two reasons; that it is simple yet comprehensive as it includes all three components of total radiation. Secondly it has been used in Lesotho by Gopinathan to study solar radiation on variously oriented surfaces [63]. In one of Gopinathan's papers where he studied radiation that is intercepted as a function of slope and azimuth in Lesotho, he commented that the Liu and Jordan model is suitable for use in Lesotho and that the mean percentage error (MPE) for this model falls within 3% [59]. Equation 2.6 was therefore used to determine the incident radiation on a tilted collector at each of the 169 grid points covering Lesotho.

3.3.2. Inputs and Assumptions

The values for global radiation I and diffuse radiation I_d were extracted directly from the TMY data. The value for beam radiation was determined by subtracting the diffuse component from the global radiation as;

$$□ = □ - □ \qquad 3.1$$

The tilt angle □ was optimized for all latitudes from -28° to -30° by adding 5° to the absolute value of the latitude angle as;

$$□□□□□□□□□ □□□□ (□□□□□□□) = |□| + 5° \qquad 3.2$$

The author of reference [85] used the value of ground albedo □ as 0.2 for Lesotho, for the reason that there is no data available for ground albedo. The same approach was taken in this study to use a ground albedo of 0.2.

3.4.Determination of Energy Output

In order to determine the electrical energy that is injected in the grid, it is necessary to know the power output of solar modules, cable losses both on DC and AC wiring, inverter efficiency at any given time, and hence determine the final yield □ . The total energy that is injected into the grid □ , which is an input to Equation 3.9 can then be determined.by multiplying the final yield and the installed capacity of the plant □ .

3.4.1. Equations and Models

Solar Energy Output: The computed incident radiation as described in Section 3.3 was used as the radiation that is received on the solar modules □ in Equation 2.20. At each of the grid points, this equation was used to determine the power output at the terminals of the solar modules □ . Using this power output, the energy that is delivered from the solar modules for each installed kWp over a year was determined. This is called array yield □ as discussed in Section 2.6 of performance indices. The energy that is injected into the grid by the inverter □ was estimated using Equation 2.22 for the inverter power. The efficiency of the inverter was estimated using Equation 3.3 that is discussed later in this section. Since one of the focus of this study is comparing system performance for different location, this was only done considering the environmental conditions that affect how much power is available for harvesting. Performance of components like inverters,

□

transformers and wiring were assumed to be the same. Hence a global value for the ratio □ was adopted.

The inverter power □ was then used to determine the electrical energy that is injected into the grid per installed kWp, which is the final yield □ .

Solar Module Field Efficiency: The field or operating temperature of the solar modules □ was discussed in Section 2.5.1. Equation 2.19 was employed in determining the field efficiency of the solar modules. As an input to this equation, the module temperature □ was determined using the SANDIA laboratories model for module operating temperature because it includes the effects of irradiance, wind speed and type of installation (open rack, closed roof mount, etc.) on the efficiency of the solar PV modules. This model has proved to be accurate with an error of ±5°C, which results with about 3% error in power output [86].

3.4.2. Inputs and Assumptions

As discussed in tariff design options in Section 2.2, policymakers have the option to set different tariff levels for different solar PV system capacities. Following this option, different system capacities were modelled to represent different types of installations as depicted in Table 3 – 1. A similar approach is taken by policymakers in Germany and the United States of America [21], [48].

Table 3-1: Modelled System Capacities

Modelled Capacity	Represented System Type
30 kWp Roof Mounted	Residential and small scale commercial roof top system of up to 100 kWp
30 kWp Ground Mounted	Residential and small scale commercial systems mounted on the ground with capacity of up to 100 kWp
500 kWp Roof Mounted	Commercial scale roof mounted systems with capacity between 100 kWp to 1,000 kWp
500 kWp Ground Mounted	Commercial scale systems mounted on the ground
10,000 kWp Ground Mounted	Utility scale systems that are installed on the ground

The following assumptions were made to some inputs in the determination solar PV output;

Modelled PV array: The PV array was modelled using the Canadian Solar Superpower CS6K – 300MS. The values for cell temperature coefficient □, the module rated efficiency □ were taken from the manufacturer datasheet. A summary of the datasheet has been provided in Table 3–2.

Table 3-2: Specifications for Canadian Solar Superpower CS6K 300MS Source [87]

Solar Module	
Name	Canadian Solar Superpower CS6K – 300M

Performance Under STC	
Maximum Power P_{max}	300 W
Open Circuit Voltage V_{oc}	39.7 V
Maximum Power Point Voltage V_{mp}	32.5 V
Short Circuit Current I_{sc}	9.83 A
Maximum Power Point Current I_{mp}	9.24 A
Efficiency	18.33%

Annual Degradation: An annual degradation d of 0.5%, which was found to be a median value in reference [73] was assumed. Annual degradation is used to reduce the electrical energy that is injected into annually by an assumed value to cater for the declining performance of the solar modules over the years in operation.

Losses: The impact of impurities on the surface of solar modules and their impact on the performance of solar PV systems were discussed in Section 2.52. An annual value for miscellaneous losses was assumed to be 1.0%.

Inverter Efficiency: The model used a KACO Powador 60.0 TL grid tie inverter. The specifications for the inverter as shown in Table 3-3;

Table 3-3: Specifications for KACO Powador 60.0 TL Source [88]

DC Input	
Operating Range	200 V – 950 V
No Load Voltage	1 000 V
Max. Input Current	3 × 36A
AC Output	
Rated Output	49 990 VA
Rated Current	3 × 72.2A
Rated Frequency	50 Hz/60 Hz
Number of Grid Phases	3
Mechanical Data	

Dimensions (H×W×D)	1 360×840×355
Weight	173 kg

The inverter efficiency was modeled with a curve fitting method based on the efficiency curve on its data sheet. A similar method has been used by reference [89]. From this method, the inverter efficiency was found to follow the following equations;

$$\eta = \begin{cases} 1200.4\eta^3 - 145.09\eta^2 + 6.5411\eta + 0.8495, & 0.01 \le \eta \le 0.055 \\ 5.2196\eta^3 - 2.9834\eta^2 + 0.5723\eta + 0.9399, & 0.055 < \eta \le 0.301 \\ 0.0109\eta^2 + 0.0022\eta + 0.9783, & 0.301 < \eta \le 1 \end{cases} \quad 3.3$$

The parameter η in Equation 3.6 represents the relative output of the inverter, defined as the instantaneous power output divided by rated power output; $\eta = \frac{P_{AC}}{P_{rated}}$.

The original efficiency curve from the manufacturer data sheet has been depicted in Figure 3–1. The resulting curve from this inverter efficiency model has been depicted in Figure 3–2.

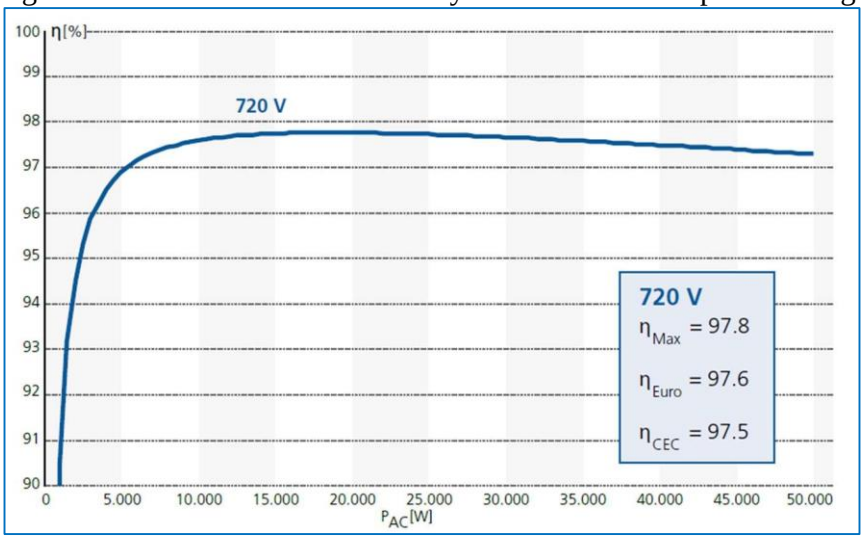

Figure 3-1: Inverter Efficiency from Datasheet Source: [88]

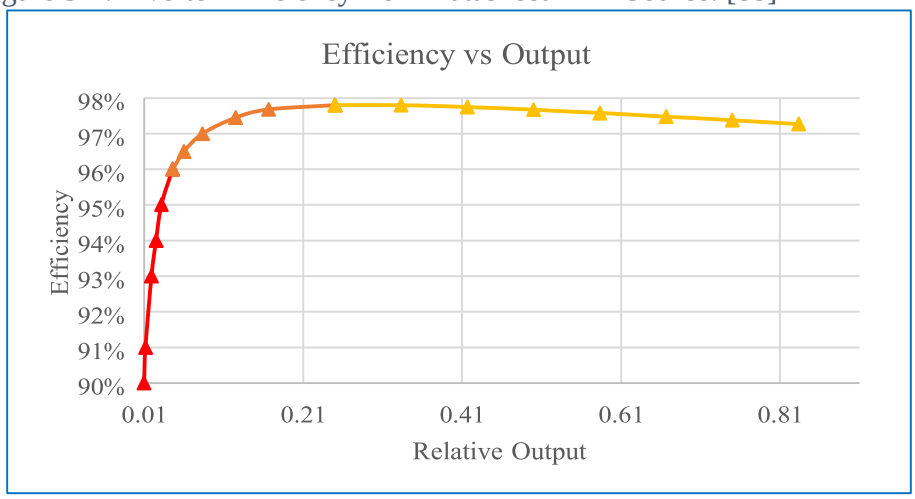

Figure 3-2: Modelled Inverter Efficiency Source: Author

3.5. Bilinear Interpolation

It is a desire especially for private developers to know the characteristics of the prospective development sites in terms of how much solar energy is available for harvesting. Our method for gridding and determining the annual array output at 0.25° intervals on latitudes and longitudes leaves vast amount of area in between the grid points un-catered for. The technique of bilinear interpolation hence becomes instrumental in determining the annual array yield in between the grid points. A model was constructed in such a way that a user can input the coordinates for a desired location and the annual array yield be automatically computed.

3.6. Zoning

For the reason that different locations have different solar resource and other factors that can affect the performance of solar modules, it is not unusual that the annual array yield would differ for different geographical regions. Setting a similar tariff for all regions implies that developers may be over-compensated in high yielding regions, while it would be the direct opposite for low yielding regions. In order to avoid this setback, high yielding regions should ideally have lower tariff than the low yielding regions. In this study, Lesotho was divided into two regions, one as high yield region and the other as low yield region. The reason for choosing to divide into only two regions is that Lesotho is not a geographically sizeable country and that two regions are easily manageable for

policy making. The procedure to achieve this was to take the highest and lowest values of annual array yield within Lesotho, represented by □ _ and □ _ respectively. The mid-point between these two values □ _ was found using Equation 3.4;

$$\square_{\_} = \square_{\_} + \frac{\square_{\_} - \square_{\_}}{2} \quad 3.4$$

Further to have two classifications of high yield regions and low yield regions Equations 3.5 and 3.6 were applied;

$$\square_{\_} = \square_{\_} + \frac{\square_{\_} - \square_{\_}}{2}\Big) \quad 3.5$$

$$\square_{\_} = \square_{\_} + \frac{\square_{\_} - \square_{\_}}{2} \quad 3.6$$

Where □ _ is the value of array yield representing high yield regions and □ _ is the value of array yield representing low yield regions.

Since the final yield □ is used as the input into the financial model to determine the feed-in tariff, the same procedure was taken to determine the final yield for high and low yield regions, □ _ and □ _ respectively.

3.7.Determination of Feed-In-Tariff

To determine the cost-reflective tariff, an LCOE methodology presented in reference [90] was employed. By this method the general approach is to determine the price for selling electricity that is reasonably above generation costs which will provide returns to invested equity capital. In order to achieve this goal, the policymaker sets a target IRR for equity, which is assumed to be the maximum that equity investors would want for their invested capital. A feed-in-tariff is then determined by setting a price that will give the equity NPV equal to zero. Any interest rate below the target IRR would then yield a positive equity NPV. While constructing a financial model for this study, the NREL Cost of Renewable Energy Spreadsheet Tool [91] and the Regulatory Framework for the Development of Renewable Energy Resources in Lesotho by the LEWA [13] were studied. Both these policy instruments use the approach to set a feed-in-tariff based on a

targeted equity IRR. Another study was also considered in constructing the financial model, which is a comparative study of the cost of electricity under different ownership structures in the United States [92].

3.7.1. Equations and Models

The FiT remuneration depends on the payment model that is used. There are two main types of payment models for FiT, namely market dependent and market independent models [44]. In market independent models, the producers are paid a fixed price that is not influenced by electricity market price, while in market dependent models, the remuneration price is set based on the electricity market price plus a specified premium [44]. Between these two, the market independent models are more predominant than market dependent models [23]. The market independent models use the Levelized Cost of Electricity (LCOE) approach to determine the FiT , in which the price of selling electricity is based on the cost of generation with an option to adjust the price for inflation [44]. Inflation adjusted FiT prohibits the decline in real value of project revenue over its lifetime, useful especially in developing countries with high level of inflation [21], [44].

In order to determine a cost reflective FiT, the payments are based on the cost of generation [22], often referred to as the LCOE [17] LCOE is defined as the unit cost of energy that will result in project revenue over its economic life being equal the Total Life Cycle Cost (TLCC) when a certain discount rate r is applied to the base year [90]. TLCC are the costs incurred for operation and maintenance of an asset in its lifetime [90]. The expression for TLCC is given by Equation 3.7 [90];

$$\square\square\square\square = \frac{\square}{(1 + \square)} \qquad 3.7$$

Where:

$\square$ is the total cost in period t; investment costs, O&M costs, replacement costs, salvage value
T is the period of analysis r is the annual discount rate

By breaking down total costs $\square$ into its individual components and equating the expression for TLCC to the revenue, the equation for LCOE becomes Equation 3.8 [93];

$$\frac{\square\square\square\square}{\square} \times \square\,(1-\square) = \frac{(\square+\square+\square+\square+\square)}{3.8\,(1+\square)} \quad (1+\square)$$

Where;

□□□□ is the levelized cost of electricity

T is the period of analysis r is the annual discount rate

□ is the annual energy production

□ is the degradation rate

□ is the investment costs

□ is the operation costs

□ is the maintenance costs

□ is the fuel cost

□ is the corporate income tax

The total revenue over the lifetime of a project and its total life cycle costs are represented by the left hand and right hand side of Equation 3.8 respectively [90]. When LCOE is adjusted to a desired FiT so that the lifetime revenue surpasses the lifetime costs, the difference between the revenue and costs in Equation 3.8 becomes the profit as given by Equation 3.9 [94], [95];

$$\frac{\square\square\square}{(1+\square)} \times \square\,(1-\square) - \frac{(\square+\square+\square+\square+\square)}{(1+\square)} = \frac{\square}{(1+\square)} \qquad 3.9$$

Where;

□ is the annual gross profit for year t

□□□ is the unit price of electricity

The rest of the terms retain the same meaning as in Equation 3.8.

The inputs for Equation 3.9 for calculation of FiT are as follows;

Investment costs, I_t

Investment costs are costs that are incurred by the project before operation, or other investments made during its lifetime for maintenance, replacement or reinforcement. Investment costs include

feasibility, engineering, purchase of equipment, land acquisition, grid connection and interest during construction [96].

Operating Costs, O_t and Maintenance Costs, M_t

Operating and maintenance costs for a project are expenses incurred for day-to-day running of the project and its maintenance and replacement of parts. Operating and maintenance costs include labour, scheduled and unscheduled maintenance, insurance and communication [96].

Fuel Costs, F_t

Fuel is part of the variable costs [96] Fuel like diesel is required for running of some energy plants, but it is not required for solar PV plants [93], [96].

Income Tax, T_t

Corporate income tax is a share of company income that is paid to the government [97].

Annual Operating Profit, P_t

The operating profit P_t is the difference between the revenue received from selling electricity and the costs in a year [94].

Annual Electricity Generation, S_t

Annual electricity generation S_t is the rated electricity output of the renewable plant in a year [93]. Annual electricity generation is discussed in detail in Sections 2.5 and 2.6.

Annual Degradation Rate, d

Degradation rate is the percentage decline in performance of solar modules over time [73]. Degradation of solar modules is discussed in detail in Section 2.6.3.

Annual Discount Rate, r

Discount rate is the opportunity cost of money invested as capital in a project [98]. The cost of capital is important in calculating FiT because it is common for renewable energy projects to secure financing through equity and loan [99]. For interest rate r in Equation 3.9, the Weighted Average Cost of Capital (WACC) is often used as the discount rate to reflect costs of loan capital and equity capital [99], [100]. Equation 3.10 depicts the formula for calculating WACC;

$$\square\square\square\square = \frac{\square}{\square + \square} \times \square + \frac{\square}{\square + \square} \times \square \qquad 3.10$$

Where;

E is equity amount

□ is the rate of return on equity

D is the debt amount

□ is the interest rate on debt

Using the LCOE method to calculate FiT, policy makers base the FiT on LCOE plus a certain premium that will allow for a predetermined internal rate of return (IRR) for equity investors [21]. To understand IRR a brief discussion of the Net Present Value (NPV) is necessary. NPV is the value of an asset or a project, measured by its discounted future cash flows, both negative and positive, versus the life cycle costs [101]. NPV is one of many matrices used for project evaluation. If NPV is positive (above zero), it means the project is worth investing in, otherwise other alternatives should be considered [102]. Equation 3.11 gives an approach to determine the NPV of a project [101];

$$\square\square\square = \frac{\square}{(1 + \square)} \qquad 3.11$$

Where;

T is the number of periods for analysis,

□ is the cash flow for period t, r is the interest rate

In Equation 3.11, the interest rate r which yields NPV = 0 is known as the IRR [101]. Figure 3 - 3 shows a demonstration of the NPV and IRR. In this illustration the IRR is the value of interest rate which crosses the horizontal axis, at NPV = 0. In this case the IRR is 15.37%.

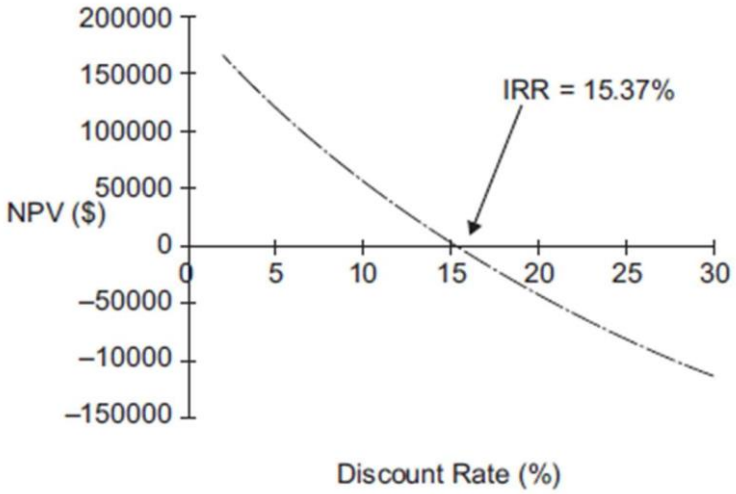

Figure 3-3: Illustration of the Internal Rate of Return Source [102]

Equation 3.9 which determines the feed-in-tariff based on the life cycle cost of generation was applied. The interest rate r that is applied depends on the cash flow in question. Cash flow to the projects, which is the Cash Available for Debt Service (CADS), after deducting corporate income tax, is evaluated using interest rate as the weighted average cost of capital (WACC). Cash flow to equity investors is evaluated using the targeted IRR. For determination of WACC, Equation 3.10 was applied. For evaluation of cash flow to the project and to equity investors using the NPV approach, Equation 3.11 was applied.

3.7.2 Inputs and Assumptions

Financing Structure: A project finance structure was used in which money lenders are paid from the income that is generated by the project [103]. It is common for large scale infrastructure projects to apply this type of financing. Two main sources of capital are loan from lenders and equity from investors [92]. For this study, a loan to equity ratio of 70:30 was assumed.

Discount Rate: As discussed briefly in Section 3.7.1, a discount rate that is applied to cash flow depends on the cash flow in question. The following financial assumptions were made regarding interest rates;

Table 3-4: Assumed Interest Rates

Interest Rate	Assumed Value
Annual Interest Rate on Loan	9%
Cost of Equity (Target equity IRR)	16%
WACC	11.10%

The 16% cost of equity was used as the maximum assumed return on investment that private investors would look for from a project. With this cost of equity, the unit price of electricity was then assumed which would give an equity NPV of zero. Any lower cost of equity lower than the assumed one would yield a positive equity NPV.

Company Tax Income: In Lesotho the income tax collected from business is called Company Income Tax (CIT). A CIT rate of 25% is applied on gross income for all businesses with the exception of manufacturing and subsistence farming [104].

Investment Costs: In Section 2.3 the costs for installation of solar PV plants were discussed. It was pointed out that the global weighted average cost for installing utility scale solar PV plants was as low as USD 1,210/kW. NREL's 2018 quarter 1 solar PV costs benchmark report reveals that the cost of installing utility scale solar PV plants was as low as USD 1,440/kWac. The report further breaks down the investment costs into soft costs, balance of system hardware, inverter and modules [48]. In this study, a similar approach to break down the investment costs was followed for different types of installations as shown in Table 3 – 5;

Table 3-5: Breakdown of Installed Costs

	30 kW Roof Mount	500 kW Roof Mount	10,000 kW Roof Mount	30 kW Ground Mount	500 kW Ground Mount	10,000 kW Ground Mount
Feasibility ($/W)	0.03	0.03	0.03	0.03	0.03	0.03
Engineering & Development ($/W)	0.15	0.12	0.1	0.12	0.11	0.1
Solar Modules ($/W)	0.8	0.8	0.6	0.8	0.8	0.6
Inverter ($/W)	0.15	0.11	0.08	0.15	0.08	0.08
Mounting Structure ($/W)	0.11	0.09	0.08	0.1	0.08	0.06
Other BoS ($/W)	0.6	0.5	0.4	0.6	0.4	0.3
Licensing ($/W)	0.02	0.02	0.02	0.02	0.02	0.02
TOTAL	1.86	1.67	1.31	1.82	1.52	1.19

Depreciation: A straight line depreciation that yields a salvage value of zero for the duration of the economic life of the project was assumed.

Other Economic and Financial Inputs and Assumptions: Other assumed economic and financial inputs have been summarized in Table 3 – 6;

Table 3-6: Economic and Financial Assumptions

Economic/Financial Parameter	Assumed Value
Loan Tenor	18 years
Duration of FiT	20 years
O&M annual escalation	1.5%

4. RESULTS

The results of the study are presented in this section. First the performance indices that are used to compare performance of systems for different locations are presented. The results for proposed feed-in tariff and other financial results are also presented. In the results, discussion and conclusion sections, the terms high yield and low yield are used to refer to high and low annual array yield as per classification in Section 3.6.

4.1. Performance Indicators

The performance indicators for the modelled systems are necessary to present in order to compare the modelled system with other systems in Lesotho or elsewhere in order to verify the model. In this section, the performance of indicators that are presented. The performance indicators will be presented for both high yield and low yield regions. The representative values for high yield and low yield regions were determined using the method as described in Section 3.6. The array yield and final yield will thus be presented as the representative values for both regions. Table 4-1 presents the results of the performance indicators;

Table 4-1: Results for Performance Indicators

Performance Indicator	High Yield Region	Low Yield Region
Array Yield Range (kWh/kWp)	1,826-1,992	1,660-1,826
Representative annual Array Yield (kWh/kWp)	1,909	1,743

Representative annual Final Yield □ (kWh/kWp)	1,885	1,713
Capacity Factor (%)	21.52	19.55

The resulting contour map of annual array yield □ , constructed using the software Surfer, has been shown in Figure 4-1;

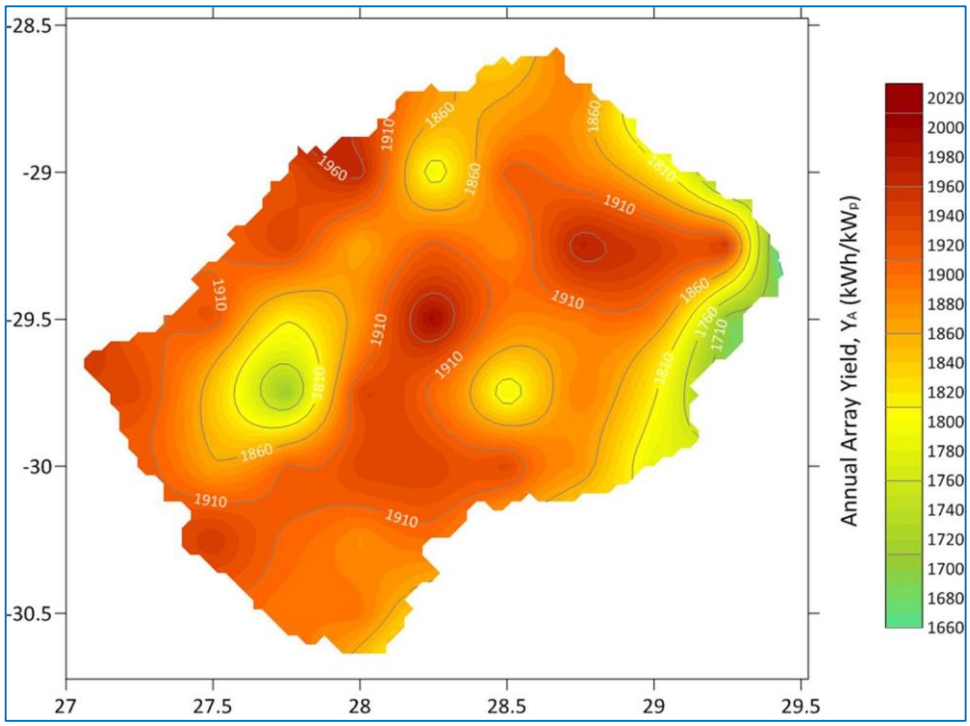

Figure 4-1: Map of Annual Array Yield, Y_A for Lesotho Source: Author

The map in Figure 4 – 1 shows the annual array yield Y_A for different locations in Lesotho. This map can be used to determine areas for potential solar PV development by looking at how much a system installed at one location can potentially yield in a year. The areas shaded in green have relatively low array yield, while areas shaded in brown have relatively high array yield. Since a value for annual array yield cannot be directly extracted from this map, bilinear interpolation becomes useful in such cases, where coordinates of a potential development site can be fed into the model and the resulting annual array yield of the site be obtained.

4.2. Zoning

Using the method described in Section 3.6, Lesotho was divided into two regions based on annual array yield □ . One region is the high yield region represented by □ _ and the low yield region which is represented by □ _ . Annual array yield was used for classification of the two regions, while the

corresponding final yields were used as input into the financial model used to determine the feed-in tariff in the respective regions. Table 4-2 shows the representative values for annual array and final yields for high and low yield regions;

Table 4-2: Table of Array and Final Yields for High and Low Yield Regions

Region	Array Yield Range (kWh/kWp)	Array Yield, □□ (kWh/kWp)	Final Yield, □□ (kWh/kWp)
High Yield	1,826-1,992	1,909	1,885
Low Yield	1,660-1,826	1,743	1,713

4.3. Financial Results

The results for the feed-in tariff for high and low yielding regions, cash flows and other financial indicators are presented in this section. First a summary of the feed-in tariffs is presented in Table 4-3;

Table 4-3: Results for FiT

System Category	FiT ($/kWh)	
	Low Array Yield Region	High Array Yield Region
30 kWp Roof Mount	0.1778	0.1616
500 kWp Roof Mount	0.1597	0.1451
30 kWp Ground Mount	0.1740	0.1581
500 kWp Groun Mount	0.1453	0.1321
10 000 kWp Ground Mount	0.1138	0.1034

4.3.1. Financial Results for Utility Scale Systems

The feed-in tariff for 10 000 kWp solar PV system which represents all ground mounted systems equal or larger in capacity than 1,000kWp was found to be USD 0.1034 in high yield regions and USD 0.1138 for low yield regions. The capital requirement for this system is USD 1,190/kWp. The project cash flow and equity cash flow for 10 000 kWp solar PV system have been depicted in Figure 4-2 and 4-3. The resulting Project NPV and IRR from the model were found to be USD 29,000 and 11.14% respectively. For equity cash flows, the resulting NPV and IRR were USD 0

and 16% respectively. The results for equity cash flow are not surprising because they were deliberately targeted in order to determine the feed-in tariff. These results for NPV and IRR also apply for low yield region. The results show that for this utility scale category, the annual cash flow for the project ranges from USD 1.1790 million to $1.664 million, while it ranges from USD 0.27 million to USD 1.194 for equity cash flow.

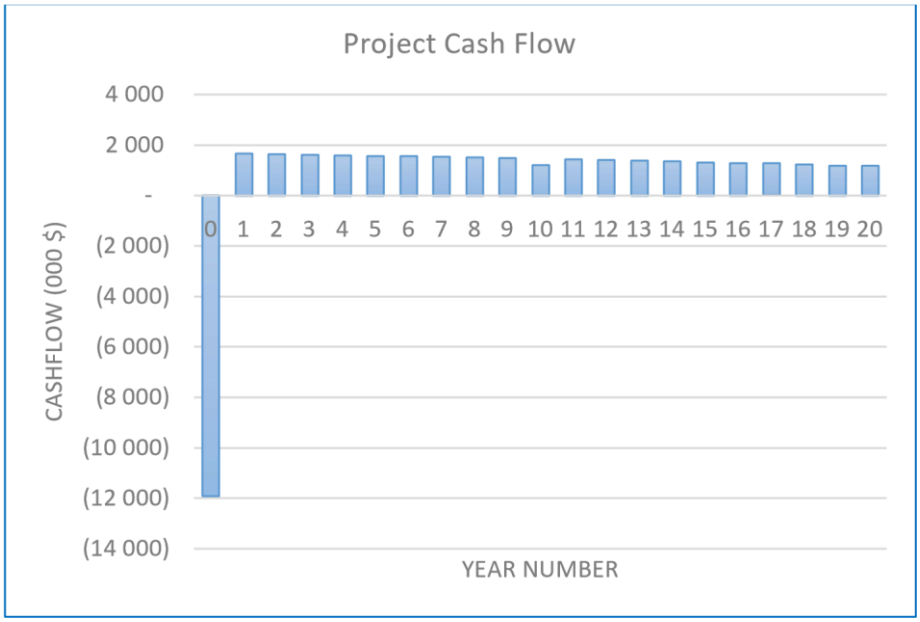

Figure 4-2: Cash flows for the Project for Utility Scale Systems Source: Author

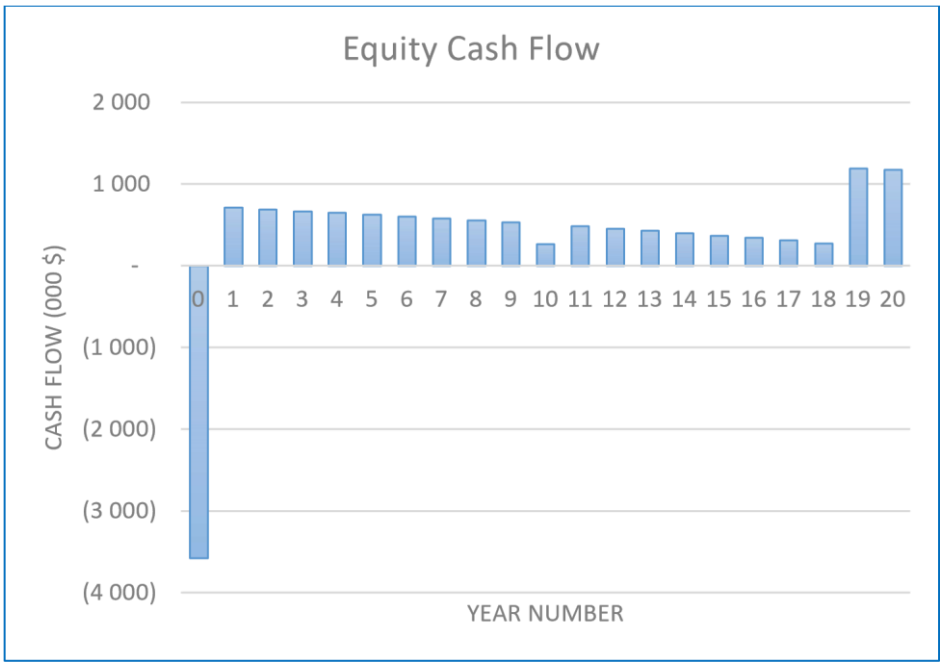

Figure 4-3: Cash flows for Equity for Utility Scale Systems Source: Author

4.3.2. Financial Results for Commercial Scale Systems

A 500 kWp system in the financial model represents all commercial system, ground mount and roof mount from 100 kWp to 1 000 kWp. The feed-in tariff for ground mount commercial systems was determined to be USD 0.1453 for low yield region and 0.1321 for high yield regions. For roof mounted systems the feed-in tariff was determined to be USD 0.1451 and USD 0.1597 for high yield and low yield regions respectively. The model shows that ground mounted systems require less capital than the roof mounted system, with their capital requirement at USD 1,520/kWp, while roof mounted systems would require USD 1,670/kWp. The resulting net present values for project NPV for ground mount and roof mount systems USD 1,835 and USD 2,035 respectively. Figure 4-4 and 4-5 show project cash flow and equity cash flow respectively for ground mount systems. The project cash flow ranges from USD 75 318 to USD 106 247 per annum, while the cash flows range from USD 17,259 to USD 76,263 per annum.

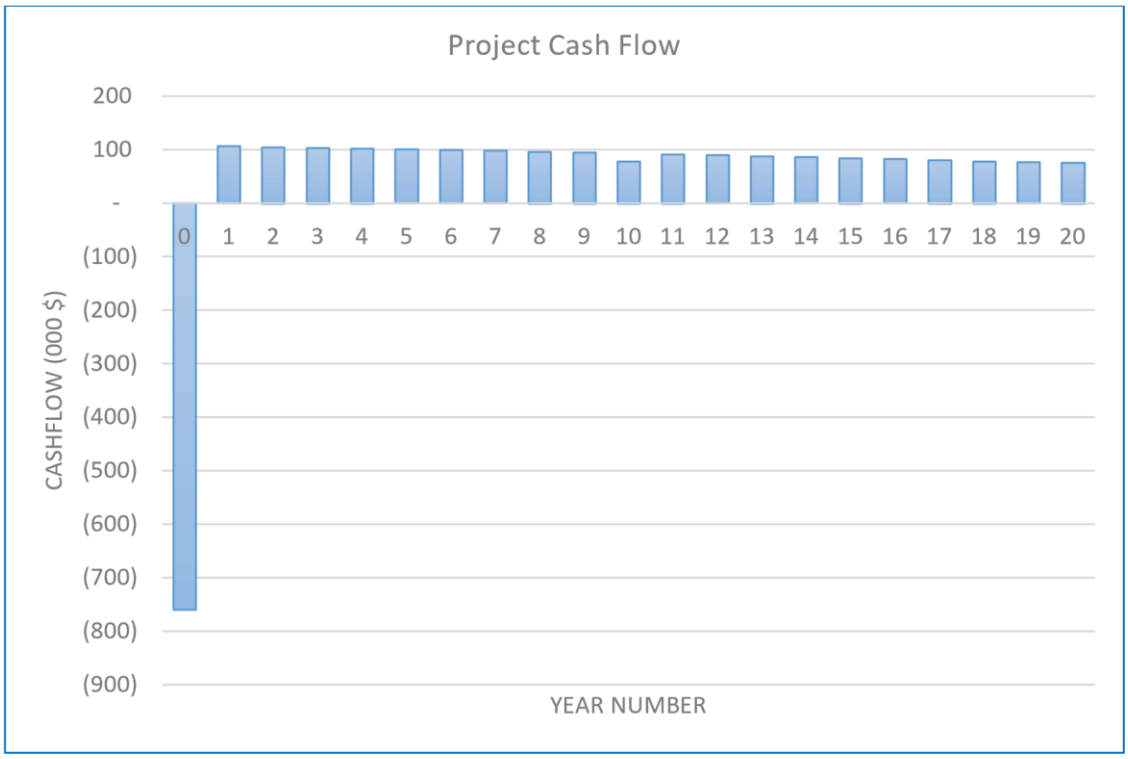

Figure 4-4: Cash flow for Project for Commercial Scale Systems Source: Author

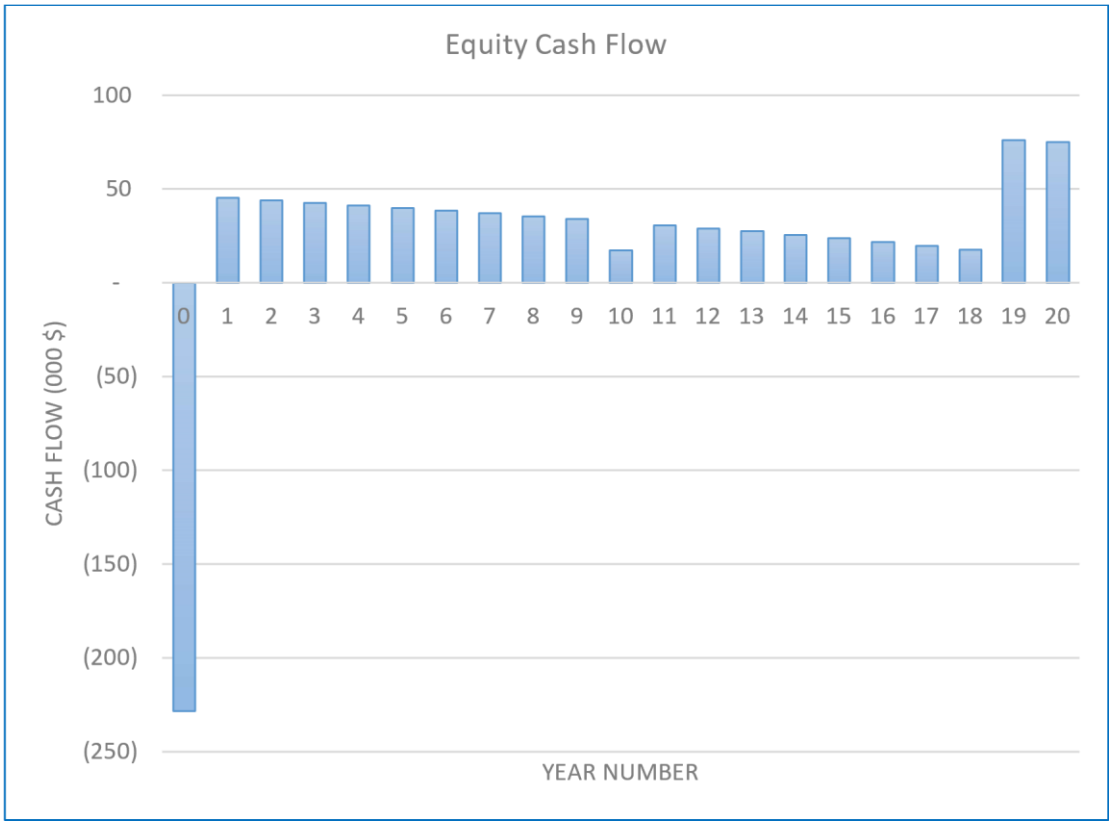

Figure 4-5:Cash flows for Equity for Commercial Scale Systems Source: Author

The cash flows for roof mount systems are not far from cash flows for ground mount systems. Cash flows for the project ranges from USD 83,750 to USD 117,761 per annum. On the other hand cash flows for equity range from USD 18,963 to USD 50,000 per annum. Figures 4-6 and 4-7 show the cash flows for project and equity respectively for roof mount commercial scale systems.

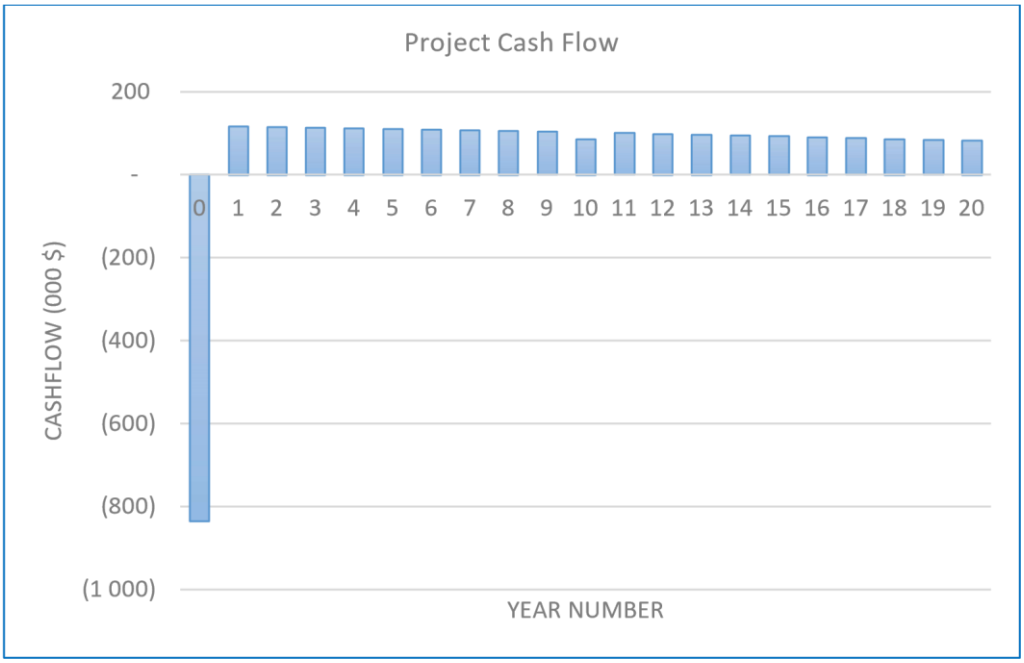

Figure 4-6:Cash flow for Project for Commercial Scale Systems Source: Author

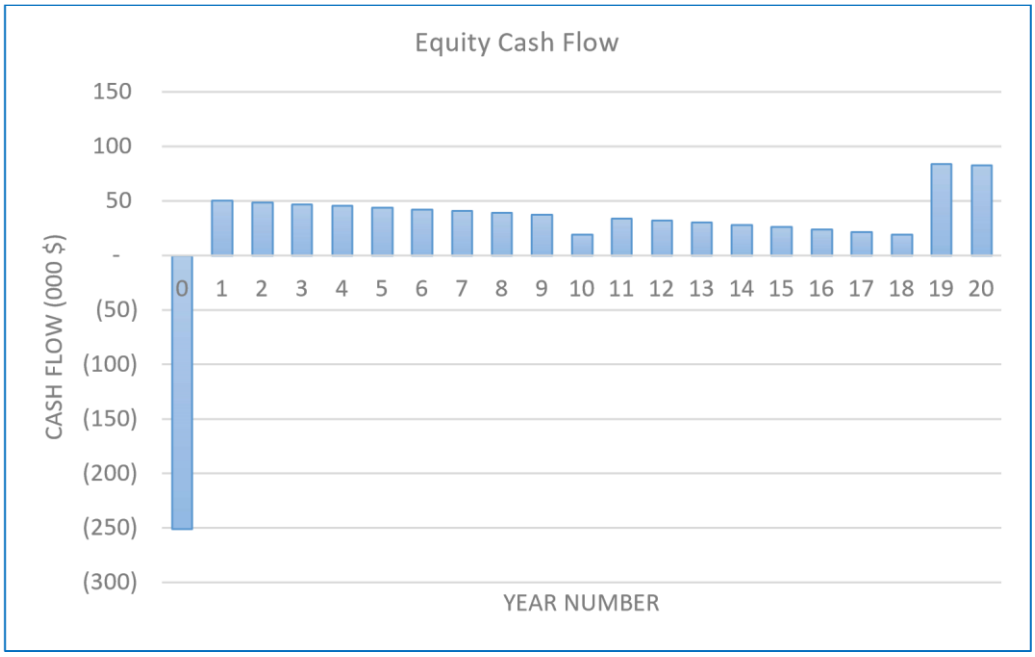

Figure 4-7: Cash flows for Equity for Commercial Scale Systems Source: Author

4.3.3. Financial Results for Residential and Small Scale Commercial Systems

In this section of the results the financial results for residential and small scale commercial systems are presented. The representative system for this category is a 30 kWp system for both ground and roof mount systems, representing systems of up to 100 kWp in installed capacity. The feed-in tariff for high yield region was determined to be USD 0.1581 and USD 0.1616 for ground mount and roof mount systems respectively. For low yield region these values were found to be USD 0.1740 and USD 0.1778 for ground mount and roof mount systems respectively. The capital requirements for 30 kWp ground mount system was found to be USD 1,820/kWp and for roof mount systems it was found to be USD 1,860/kWp. The cash flow for this system in roof mount category both for the project and equity have been shown in Figures 4-8 and 4-9 show the cash flow for project and for equity for residential scale systems in roof mount category. The results show that the Project NPV would be USD 136 for roof mount systems and USD 133 for ground mount systems. The resulting cash flow for roof mount category for the project ranges from USD 5,530 to USD 7,803 per annum, while equity cash flow in the same category ranges from USD 1,300 to USD 5,600 per annum.

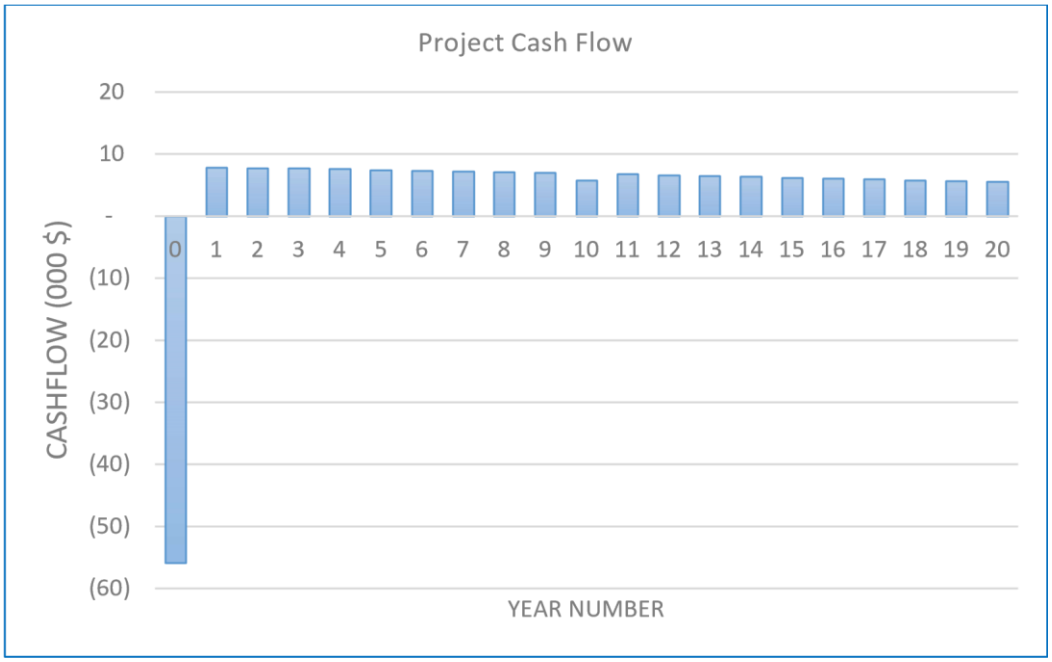

Figure 4-8:Cash flow for the Project in Roof Mount Residential Scale Systems Source: Author

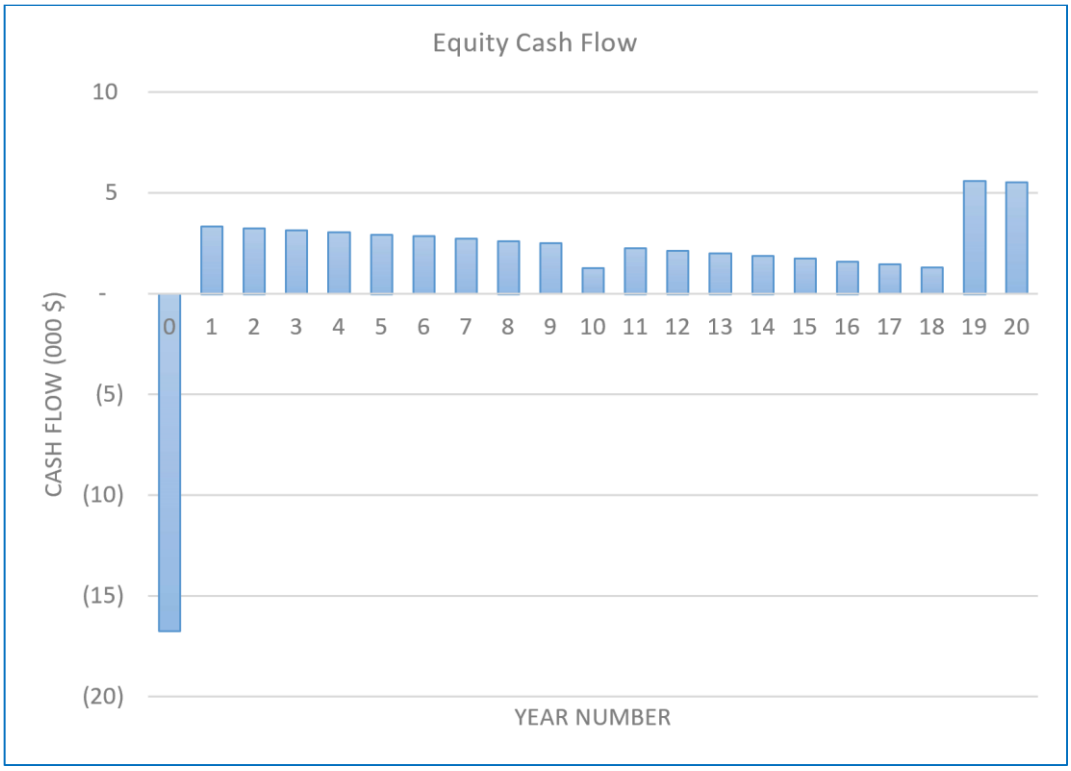

Figure 4-9: Cash flows for Equity in the Roof Mount Residential Scale Systems Source: Author

In this residential and small scale commercial systems, the financial results show that the project cash flow for ground mount systems would range from USD 5,411 to USD 7,635 per annum. Cash flow for equity in the same category would range from USD 1,272 to USD 5,479 per annum. Figures 4-10 and 4-11 show cash flows for the project and equity respectively;

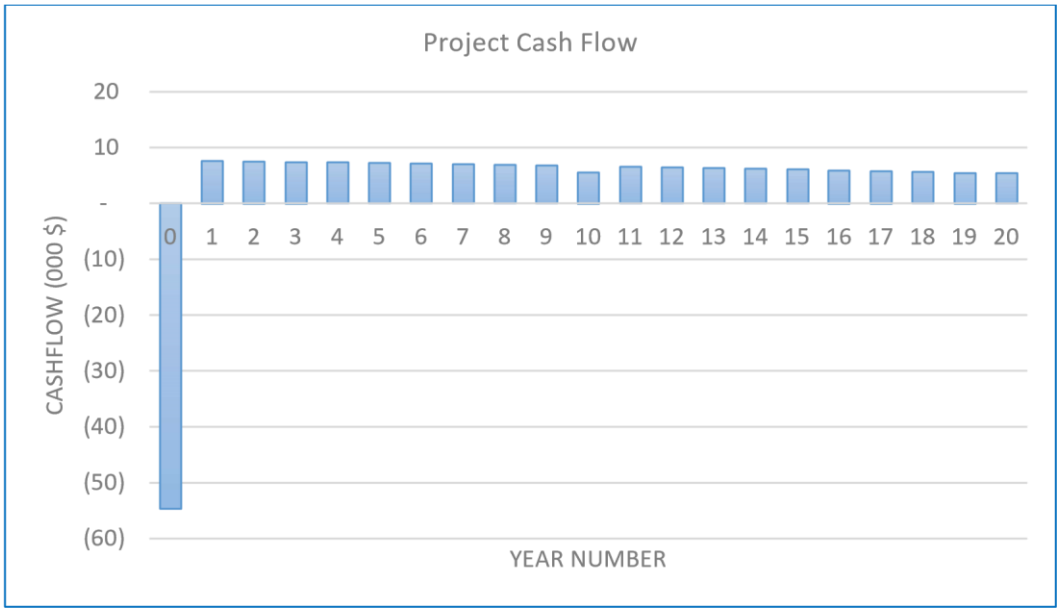

Figure 4-10: Cash flow for Project in the Ground Mount Residential Scale Source: Author Systems

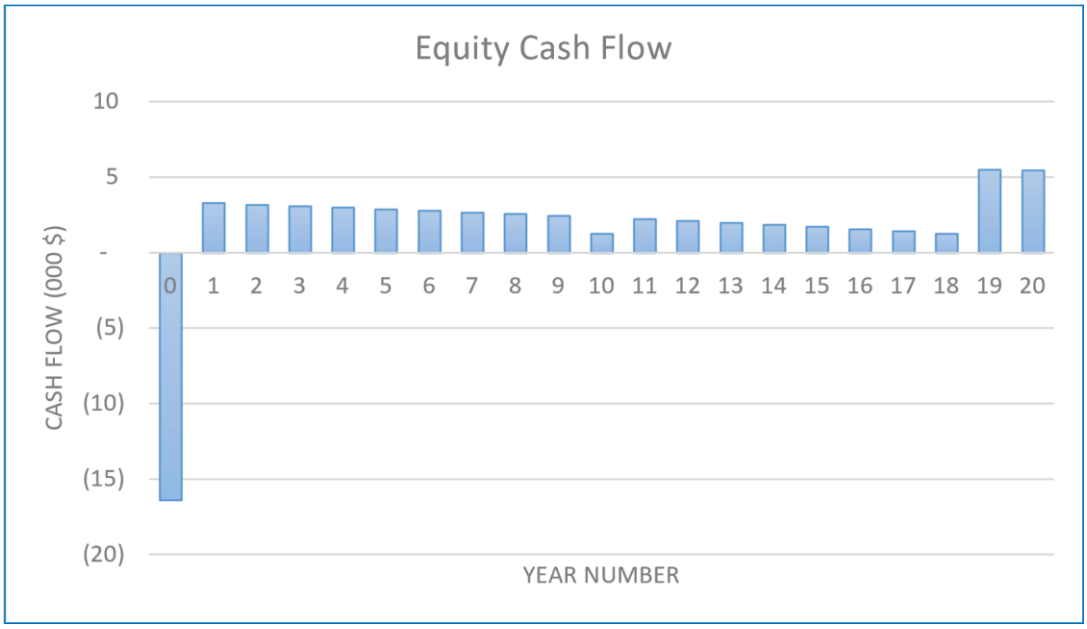

Figure 4-11: Cash flow for Equity in the Ground Mount Residential Scale Systems Source: Author

5. DISCUSSION

The financial results show that by setting different tariffs for locations with different resources, the same economic impact can be achieved. For example, looking at the utility scale system, setting USD 0.1034 for high yield region and USD 0.1138 for low yield regions as the feed-in tariff yields a project NPV of USD 29,000 in both cases. Another perspective of looking into this issue is to observe at how certain regions, would perform if only one tariff was adopted for all regions. In order to perform this evaluation we used the maximum annual final yield which is 1,970 kWh/kWp. The resulting feed-in tariff was found to be USD 0.0989. Using this value of feed-in tariff for the lowest yielding region, which is 1,628 kWh/kWp results in a project NPV of USD 1.86 million and equity NPV of USD -1.43 million. This means the projects in low yielding regions would not attract investment and defeat the whole purpose of the feed-in tariff policy.

In order to ensure economic and financial sustainability of projects under feed-in tariff, setting the feed-in tariff based on an assumed IRR for equity investors can make this achievement. This means in the financial model, a certain IRR is set which is assumed to be the maximum hurdle rate for equity investors. A tariff that will give the equity NPV as zero is then set at the desired feed-in tariff. Since the IRR would be the maximum that equity investors look for, any discount rate or interest rate below the IRR would yield a positive NPV, which would make the project worth investing in.

5.1.Policy Implications

Policymakers have to be aware of the importance of setting different tariffs for differently yielding regions as already discussed. The same reasoning applies for setting different tariffs for different eligible capacities. Ground mount and roof mount systems have different specific investments costs (in $/KW). As already seen, in the case of this study, looking at the commercial scale systems, the investment costs for ground mount systems is USD 1,520/kWp while it is USD 1,670/kWp for roof mount systems. Again in order to achieve the same economic impact for these differing systems, different tariffs need to be considered.

5.2.Limitations

The main limitation of this study is the use of TMY data. While it is desirable to use ground measured data for studies like this one, the reason for using TMY data is for its availability in a $0.25° \times 0.25°$ grid, data which is otherwise not available.

6. CONCLUSIONS AND RECOMMENDATIONS

To conclude, this study makes the following recommendations;

The study recommends the following feed-in tariffs for grid connected solar PV systems; Table 6-1: Recommended FiT for Grid Connected Solar PV Systems

System Category	FiT ($/kWh)	
	Low Array Yield Region	High Array Yield Region
30 kWp Roof Mount	0.1778	0.1616
500 kWp Roof Mount	0.1597	0.1451
30 kWp Ground Mount	0.1740	0.1581
500 kWp Groun Mount	0.1453	0.1321
10 000 kWp Ground Mount	0.1138	0.1034

Location-Specific FiT: A location specific feed-in tariff for solar PV systems is recommended based on the annual array yield. A methodology to divide Lesotho into two regions has been presented in this study. However the methodology to do so should not be limited only to the one presented here, but other methodologies may be explored.

Size-Specific FiT: Capital costs may differ significantly for common types of installations. In this study two types of installation were presented which are ground mount and roof mount installations. Setting a different tariff for different types of installation is recommended that can achieve the same economic impact for different systems.

FiT Duration: 20 years for feed-in tariff is recommended. This is the most commonly used duration for solar PV plants across the globe. Shorter periods may see much higher feed-in tariffs, while longer periods may go beyond the useful economic life of components in the solar PV system.

Inflation Indexed Tariff: For manageability, a fixed feed in tariff is recommended. However the impacts of inflation must be carefully considered by indexing other variables like the annual O&M costs to inflation in the financial model.

Other recommendations: It is recommended that a maximum capacity for solar PV systems that will fall under FiT scheme be set. This will allow other mechanisms, particularly tendering schemes to be part of the energy procurement policies.

7. REFERENCES

[1] M. Senatla, M. Nchake, B. M. Taele, and I. Hapazari, "Electricity capacity expansion plan for Lesotho – implications on energy policy," Energy Policy, vol. 120, pp. 622–634, Sep. 2018, doi: 10.1016/j.enpol.2018.06.003.

[2] "Lesotho Electricity and Water Authority Annual Report 2018/2019," Lesotho Electricity and Water Authority, Maseru, Lesotho, 2019.

[3] B. M. Taele, L. Mokhutšoane, I. Hapazari, S. B. Tlali, and M. Senatla, "Grid electrification challenges, photovoltaic electrification progress and energy sustainability in Lesotho," Renewable and Sustainable Energy Reviews, vol. 16, no. 1, pp. 973–980, Jan. 2012.

[4] "2019 Energy Report," Bureau of Statistics, Maseru, Lesotho, Statistical Report 10, 2020. [Online]. Available: http://www.bos.gov.ls/New Folder/Environment and Energy/2019_Energy_Report.zip.

[5] P. Ramanan, K. Murugavel, and K. Alagar, "Performance analysis and energy metrics of grid-connected photovoltaic systems," Energy for Sustainable Development, vol. 52, pp. 104–115, Oct. 2019, doi: 10.1016/j.esd.2019.08.001.

[6] F. Muhammad-Sukki et al., "Feed-in tariff for solar photovoltaic: The rise of Japan," Renewable Energy, vol. 68, pp. 636–643, Aug. 2014.

[7] "Renewable power generation costs in 2018," International Renewable Energy Agency, Abu Dhabi, 2019.

[8] T. Bano and K. V. S. Rao, "Levelized Electricity Cost of Five Solar Photovoltaic Plants of Different Capacities," Procedia Technology, vol. 24, pp. 505–512, 2016, doi: 10.1016/j.protcy.2016.05.086.

[9] M. Ram, M. Child, A. Aghahosseini, D. Bogdanov, A. Lohrmann, and C. Breyer, "A comparative analysis of electricity generation costs from renewable, fossil fuel and nuclear sources in G20 countries for the period 2015-2030," Journal of Cleaner Production, vol. 199, pp. 687–704, Oct. 2018, doi: 10.1016/j.jclepro.2018.07.159.

[10] T. Ntlama, "Consultation with LEWA," Jan. 09, 2020.

[11] "Lesotho Energy Policy 2015-2025," Government of the Kingdom of Lesotho, Maseru, Lesotho, Policy Document, 2015.

[12] "SADC Renewable Energy and Energy Efficiency Status Report," REN21, Paris, France, 2018. Accessed: May 13, 2019. [Online]. Available: http://www.ren21.net/wpcontent/uploads/2018/12/SADC_2018_web.pdf.

[13] "Regulatory Framework for the Development of Renewable Energy Resources in Lesotho," Lesotho Electricity and Water Authority, Maseru, Lesotho, MI1582, Sep. 2015.

[14] "Report on the Analysis of LEC Load Shedding for Period April - July 2008," Lesotho Electricity and Water Authority, Maseru, Lesotho, 2008.

[15] T. Adefarati and R. C. Bansal, "Energizing Renewable Energy Systems and Distribution Generation," in Pathways to a Smarter Power System, Elsevier, 2019, pp. 29–65.

[16] K. Cory, T. Couture, and C. Kreycik, "Feed-in Tariff Policy: Design, Implementation, and RPS Policy Interactions," NREL/TP-6A2-45549, 951016, Mar. 2009. doi: 10.2172/951016.

[17] M. Greer, Electricity marginal cost pricing: applications in eliciting demand responses. Amsterdam: Butterworth-Heinemann, 2012.

[18] A. Zahedi, “A review on feed-in tariff in Australia, what it is now and what it should be,” Renewable and Sustainable Energy Reviews, vol. 14, no. 9, pp. 3252–3255, Dec. 2010, doi: 10.1016/j.rser.2010.07.033.
[19] D. Jacobs, Renewable Energy Policy Convergence in the EU. England: Ashgate, 2012.
[20] F. Muhammad-Sukki et al., “Progress of feed-in tariff in Malaysia: A year after,” Energy Policy, vol. 67, pp. 618–625, Apr. 2014, doi: 10.1016/j.enpol.2013.12.044.
[21] M. Mendonça, D. Jacobs, and B. K. Sovacool, Powering the green economy: the feed-in tariff handbook. London ; Sterling, VA: Earthscan, 2010.
[22] T. D. Couture, K. Cory, C. Kreycik, and E. Williams, “A Policymaker’s Guide to Feedin Tariff Policy Design,” NREL/TP--6A2-44849, 1219187, Jul. 2010. Accessed: Jun. 05, 2019. [Online]. Available: http://www.osti.gov/servlets/purl/1219187/.
[23] A. Klein, B. Pfluger, A. Held, M. Ragwitz, G. Resch, and T. Faber, “Evaluation of different feed-in tariff design options – Best practice paper for the International Feed-In Cooperation,” p. 95, Oct. 2008.
[24] M. Fulton and R. Capalino, “The German Feed-in Tariff: Recent Policy Changes,” p. 27, Sep. 2012.
[25] M. T. García-Alvarez and R. M. Mariz-Pérez, “Analysis of the Success of Feed-in Tariff for Renewable Energy Promotion Mechanism in the EU: Lessons from Germany and Spain,” Procedia - Social and Behavioral Sciences, vol. 65, pp. 52–57, Dec. 2012, doi: 10.1016/j.sbspro.2012.11.090.
[26] R. Wand and F. Leuthold, “Feed-in tariffs for photovoltaics: Learning by doing in Germany?,” Applied Energy, vol. 88, no. 12, pp. 4387–4399, Dec. 2011, doi: 10.1016/j.apenergy.2011.05.015.
[27] W. H. Rickerson, J. L. Sawin, and R. C. Grace, “If the Shoe FITs: Using Feed-in Tariffs to Meet U.S. Renewable Electricity Targets,” The Electricity Journal, vol. 20, no. 4, pp. 73–86, May 2007, doi: 10.1016/j.tej.2007.03.007.
[28] S. Winter and L. Schlesewsky, “The German feed-in tariff revisited - an empirical investigation on its distributional effects,” Energy Policy, vol. 132, pp. 344–356, Sep. 2019, doi: 10.1016/j.enpol.2019.05.043.
[29] F. Muhammad-Sukki et al., “Revised feed-in tariff for solar photovoltaic in the United Kingdom: A cloudy future ahead?,” Energy Policy, vol. 52, pp. 832–838, Jan. 2013, doi: 10.1016/j.enpol.2012.09.062.
[30] L.-C. Ye, J. F. D. Rodrigues, and H. X. Lin, “Analysis of feed-in tariff policies for solar photovoltaic in China 2011–2016,” Applied Energy, vol. 203, pp. 496–505, Oct. 2017, doi: 10.1016/j.apenergy.2017.06.037.
[31] Y. Glemarec, W. Rickerson, and O. Waissbein, “Transforming On-Grid Renewable Energy Markets,” United Nation Development Programme, New York, NY, 2012.
[32] A. Pyrgou, A. Kylili, and P. A. Fokaides, “The future of the Feed-in Tariff (FiT) scheme in Europe: The case of photovoltaics,” Energy Policy, vol. 95, pp. 94–102, Aug. 2016, doi: 10.1016/j.enpol.2016.04.048.
[33] C. Morris, “Germany’s Energiewende,” in Global Sustainable Communities Handbook, Elsevier, 2014, pp. 105–113.
[34] E. V. Hobman, E. R. Frederiks, K. Stenner, and S. Meikle, “Uptake and usage of costreflective electricity pricing: Insights from psychology and behavioural economics,”

Renewable and Sustainable Energy Reviews, vol. 57, pp. 455–467, May 2016, doi: 10.1016/j.rser.2015.12.144.
[35] "National Renewable Energy Policy," Ministry of Energy and Power Development, Zimbabwe, Policy Document, Mar. 2019.
[36] M. Meyer-Renschhausen, "Evaluation of feed-in tariff-schemes in African countries," Journal of Energy in Southern Africa, vol. 24, no. 1, p. 11, 2013.
[37] J. Huenteler, "International support for feed-in tariffs in developing countries—A review and analysis of proposed mechanisms," Renewable and Sustainable Energy Reviews, vol. 39, pp. 857–873, Nov. 2014, doi: 10.1016/j.rser.2014.07.124.
[38] S. Haddoum, H. Bennour, and T. Ahmed Zaïd, "Algerian Energy Policy: Perspectives, Barriers, and Missed Opportunities," Global Challenges, vol. 2, no. 8, p. 1700134, Aug. 2018, doi: 10.1002/gch2.201700134.
[39] S. W. Ndiritu and M. K. Engola, "The effectiveness of feed-in-tariff policy in promoting power generation from renewable energy in Kenya," Renewable Energy, p. S0960148120311587, Jul. 2020, doi: 10.1016/j.renene.2020.07.082.
[40] J. Haselip, I. Nygaard, U. Hansen, and E. Ackom, Diffusion of renewable energy technologies Case studies of enabling frameworks in developing countries. Denmark: Magnum Customer Publishing, 2011.
[41] A. Eberhard, "Feed-In Tariffs or Auctions?," viewpoint, p. 8, Apr. 2013.
[42] A. Poullikkas, "A comparative assessment of net metering and feed in tariff schemes for residential PV systems," Sustainable Energy Technologies and Assessments, vol. 3, pp. 1–8, Sep. 2013, doi: 10.1016/j.seta.2013.04.001.
[43] P. Sun and P. Nie, "A comparative study of feed-in tariff and renewable portfolio standard policy in renewable energy industry," Renewable Energy, vol. 74, pp. 255–262, Feb. 2015, doi: 10.1016/j.renene.2014.08.027.
[44] T. Couture and Y. Gagnon, "An analysis of feed-in tariff remuneration models: Implications for renewable energy investment," Energy Policy, vol. 38, no. 2, pp. 955–965, Feb. 2010.
[45] A. Yatchew and A. Baziliauskas, "Ontario feed-in-tariff programs," Energy Policy, vol. 39, no. 7, pp. 3885–3893, Jul. 2011, doi: 10.1016/j.enpol.2011.01.033.
[46] Y.-H. Huang and J.-H. Wu, "Assessment of the feed-in tariff mechanism for renewable energies in Taiwan," Energy Policy, vol. 39, no. 12, pp. 8106–8115, Dec. 2011, doi: 10.1016/j.enpol.2011.10.005.
[47] "Renewable Energy Feed-In Tariff Phase 2," National Energy Regulator of South Africa, South Africa, Jul. 2009. Accessed: Dec. 21, 2019. [Online]. Available: http://www.nersa.org.za/Admin/Document/Editor/file/Electricity/REFIT%20Phase%20II% 20150709.pdf.
[48] R. Fu, D. Feldman, and R. Margolis, "U.S. Solar Photovoltaic System Cost Benchmark: Q1 2018," Renewable Energy, p. 63, 2018.
[49] M. Woodhouse, D. Feldman, R. Fu, K. Horowitz, and D. Chung, "On the Path to SunShot: The Role of Advancements in Solar Photovoltaic Efficiency, Reliability, and Costs," p. 44.
[50] "World Energy Outlook 2016," International Energy Agency, Paris, France, 2016.
[51] S. Kalogirou, Solar energy engineering: processes and systems, Second edition. Amsterdam ; Boston: Elsevier, AP, Academic Press is an imprint of Elsevier, 2014.

[52] K. Mertens and G. Roth, Photovoltaics: Fundamentals, Technology and Practice. West Sussex, United Kingdom: John Wiley & Sons, 2014.
[53] J. A. Duffie and W. A. Beckman, Solar Engineering of Thermal Processes, 4th Edition. New Jersey: John Wiley & Sons, 2013.
[54] J. Widén and J. Munkhammar, Solar Radiation Theory. Uppsala, Sweden: Uppsala University, 2019.
[55] M. A. Danandeh and S. M. Mousavi G., "Solar irradiance estimation models and optimum tilt angle approaches: A comparative study," Renewable and Sustainable Energy Reviews, vol. 92, pp. 319–330, Sep. 2018, doi: 10.1016/j.rser.2018.05.004.
[56] M. Despotovic and V. Nedic, "Comparison of optimum tilt angles of solar collectors determined at yearly, seasonal and monthly levels," Energy Conversion and Management, vol. 97, pp. 121–131, Jun. 2015, doi: 10.1016/j.enconman.2015.03.054.
[57] V. Badescu, Ed., Modeling solar radiation at the earth's surface: recent advances. Berlin: Springer, 2008.
[58] K. N. Shukla, S. Rangnekar, and K. Sudhakar, "Comparative study of isotropic and anisotropic sky models to estimate solar radiation incident on tilted surface: A case study for
Bhopal, India," Energy Reports, vol. 1, pp. 96–103, Nov. 2015, doi: 10.1016/j.egyr.2015.03.003.
[59] K. K. Gopinathan, N. B. Maliehe, and M. I. Mpholo, "A study on the intercepted insolation as a function of slope and azimuth of the surface," Energy, vol. 32, no. 3, pp. 213– 220, Mar. 2007, doi: 10.1016/j.energy.2006.04.009.
[60] R. Mubarak, M. Hofmann, S. Riechelmann, and G. Seckmeyer, "Comparison of Modelled and Measured Tilted Solar Irradiance for Photovoltaic Applications," Energies, vol. 10, no. 11, p. 1688, Oct. 2017, doi: 10.3390/en10111688.
[61] S. M. Besarati, R. V. Padilla, D. Y. Goswami, and E. Stefanakos, "The potential of harnessing solar radiation in Iran: Generating solar maps and viability study of PV power plants," Renewable Energy, vol. 53, pp. 193–199, May 2013, doi: 10.1016/j.renene.2012.11.012.
[62] D. T. Reindl, W. A. Beckman, and J. A. Duffie, "Evaluation of hourly tilted surface radiation models," Solar Energy, vol. 45, no. 1, pp. 9–17, 1990, doi: 10.1016/0038092X(90)90061-G.
[63] K. K. Gopinathan, "Solar radiation on variously oriented sloping surfaces," Solar Energy, vol. 47, no. 3, pp. 173–179, 1991, doi: 10.1016/0038-092X(91)90076-9.
[64] A. K. Yadav and S. S. Chandel, "Tilt angle optimization to maximize incident solar radiation: A review," Renewable and Sustainable Energy Reviews, vol. 23, pp. 503–513, Jul. 2013, doi: 10.1016/j.rser.2013.02.027.
[65] S. Dubey, J. N. Sarvaiya, and B. Seshadri, "Temperature Dependent Photovoltaic (PV) Efficiency and Its Effect on PV Production in the World – A Review," Energy Procedia, vol. 33, pp. 311–321, 2013, doi: 10.1016/j.egypro.2013.05.072.
[66] S. Yoshida, S. Ueno, N. Kataoka, H. Takakura, and T. Minemoto, "Estimation of global tilted irradiance and output energy using meteorological data and performance of photovoltaic modules," Solar Energy, vol. 93, pp. 90–99, Jul. 2013, doi: 10.1016/j.solener.2013.04.001.

[67] S. Chakraborty, P. K. Sadhu, and N. Pal, “Technical mapping of solar PV for ISM-an approach toward green campus,” Energy Science & Engineering, vol. 3, no. 3, pp. 196–206, May 2015, doi: 10.1002/ese3.65.
[68] D. M. Riley, C. W. Hansen, and M. Farr, “A performance model for photovoltaic modules with integrated microinverters.,” Sandia National Laboratories, Carlifonia, SAND20150179, 1504111, Jan. 2015. doi: 10.2172/1504111.
[69] B. Shiva Kumar and K. Sudhakar, “Performance evaluation of 10 MW grid connected solar photovoltaic power plant in India,” Energy Reports, vol. 1, pp. 184–192, Nov. 2015, doi: 10.1016/j.egyr.2015.10.001.
[70] D. Thevenard and S. Pelland, “Estimating the uncertainty in long-term photovoltaic yield predictions,” Solar Energy, vol. 91, pp. 432–445, May 2013, doi: 10.1016/j.solener.2011.05.006.
[71] S. K. Yadav and U. Bajpai, “Performance evaluation of a rooftop solar photovoltaic power plant in Northern India,” Energy for Sustainable Development, vol. 43, pp. 130–138, Apr. 2018, doi: 10.1016/j.esd.2018.01.006.
[72] K. Ilse et al., “Techno-Economic Assessment of Soiling Losses and Mitigation Strategies for Solar Power Generation,” Joule, vol. 3, no. 10, pp. 2303–2321, Oct. 2019, doi: 10.1016/j.joule.2019.08.019.
[73] D. C. Jordan and S. R. Kurtz, “Photovoltaic Degradation Rates-an Analytical Review: Photovoltaic degradation rates,” Progress in Photovoltaics: Research and Applications, vol. 21, no. 1, pp. 12–29, Jan. 2013, doi: 10.1002/pip.1182.
[74] A. Limmanee et al., “Degradation analysis of photovoltaic modules under tropical climatic conditions and its impacts on LCOE,” Renewable Energy, vol. 102, pp. 199–204, Mar. 2017, doi: 10.1016/j.renene.2016.10.052.
[75] E. Roumpakias and A. Stamatelos, “Performance analysis of a grid-connected photovoltaic park after 6 years of operation,” Renewable Energy, vol. 141, pp. 368–378, Oct. 2019, doi: 10.1016/j.renene.2019.04.014.
[76] T. Hove, “A method for predicting long-term average performance of photovoltaic systems,” Renewable Energy, vol. 21, no. 2, pp. 207–229, Oct. 2000, doi: 10.1016/S09601481(99)00131-7.
[77] N. M. Kumar, R. P. Gupta, M. Mathew, A. Jayakumar, and N. K. Singh, “Performance, energy loss, and degradation prediction of roof-integrated crystalline solar PV system installed in Northern India,” Case Studies in Thermal Engineering, vol. 13, p. 100409, Mar. 2019, doi: 10.1016/j.csite.2019.100409.
[78] A. Necaibia et al., “Analytical assessment of the outdoor performance and efficiency of grid-tied photovoltaic system under hot dry climate in the south of Algeria,” Energy Conversion and Management, vol. 171, pp. 778–786, Sep. 2018, doi: 10.1016/j.enconman.2018.06.020.
[79] K.-T. Chang, Introduction to geographic information systems, Ninth Edition. New York: McGraw-Hill Education, 2018.
[80] E. J. Kirkland, Advanced computing in electron microscopy, Second edition. New York: Springer, 2010.
[81] D. V. says, “Bilinear Interpolation: Resample Image Cell Size with 4 Nearest Neighbors,” GIS Geography, Dec. 10, 2017. https://gisgeography.com/bilinear-interpolation-resampling/ (accessed Dec. 26, 2020).

[82] "JRC Photovoltaic Geographical Information System (PVGIS) - European Commission." https://re.jrc.ec.europa.eu/pvg_tools/en/tools.html (accessed Oct. 22, 2019).
[83] J. Kleissl, Solar Energy Forecasting and Resource Assessment, 1. ed. Burlington: Elsevier Science, 2013.
[84] N. Martin and J. M. Ruiz, "Calculation of the PV modules angular losses under field conditions by means of an analytical model," Solar Energy Materials, p. 14, 2001.
[85] K. K. Gopinathan, "Solar radiation on variously oriented sloping surfaces," Solar Energy, vol. 47, no. 3, pp. 173–179, 1991, doi: 10.1016/0038-092X(91)90076-9.
[86] J. A. Kratochvil, W. E. Boyson, and D. L. King, "Photovoltaic array performance model.," Sandia National Laboratories, Carlifonia, SAND2004-3535, 919131, Aug. 2004. doi: 10.2172/919131.
[87] "Canadian Solar Superpower CS6K - 300MS Datasheet." Canadian Solar Inc.
[88] "Kaco Powador 60.0 TL3 Data Sheet." KACO New Energy, Accessed: Sep. 17, 2019. [Online]. Available: http://www.europesolarshop.com/document/kaco/powador/DTS_PW_30-60_TL3_en.pdf.
[89] H. A. Kazem, M. H. Albadi, A. H. A. Al-Waeli, A. H. Al-Busaidi, and M. T. Chaichan, "Techno-economic feasibility analysis of 1 MW photovoltaic grid connected system in Oman," Case Studies in Thermal Engineering, vol. 10, pp. 131–141, Sep. 2017, doi: 10.1016/j.csite.2017.05.008.
[90] W. Short, D. J. Packey, and T. Holt, "A manual for the economic evaluation of energy efficiency and renewable energy technologies," NREL/TP--462-5173, 35391, Mar. 1995. Accessed: Jun. 05, 2019. [Online].
[91] "CREST: Cost of Renewable Energy Spreadsheet Tool | Energy Analysis | NREL." https://www.nrel.gov/analysis/crest.html (accessed Jan. 28, 2020).
[92] R. Wiser and E. Kahn, "Alternative windpower ownership structures: Financing terms and project costs," LBNL--38921, 272563, May 1996. doi: 10.2172/272563.
[93] K. Branker, M. J. M. Pathak, and J. M. Pearce, "A review of solar photovoltaic levelized cost of electricity," Renewable and Sustainable Energy Reviews, vol. 15, no. 9, pp. 4470–4482, Dec. 2011.
[94] W. Muneer, K. Bhattacharya, and C. A. Canizares, "Large-Scale Solar PV Investment Models, Tools, and Analysis: The Ontario Case," IEEE Transactions on Power Systems, vol. 26, no. 4, pp. 2547–2555, Nov. 2011.
[95] C. Yang and Z. Ge, "Dynamic feed-in tariff pricing model of distributed photovoltaic generation in China," Energy Procedia, vol. 152, pp. 27–32, Oct. 2018, doi: 10.1016/j.egypro.2018.09.054.
[96] A. Pueyo, "Cost and returns of renewable energy in sub-saharan africa," p. 65.
[97] J. D. Wright, "International Encyclopedia of the Social & Behavioral Sciences," p. 25893. [98] H. Khatib, "The Discount Rate - A Tool for Managing Risk in Energy Investments," p. 2.
[99]J. Ondraczek, N. Komendantova, and A. Patt, "WACC the dog: The effect of financing costs on the levelized cost of solar PV power," Renewable Energy, vol. 75, pp. 888–898, Mar. 2015, doi: 10.1016/j.renene.2014.10.053.

[100] A. Pierru and D. Babusiaux, “WACC and free cash flows: A simple adjustment for capitalized interest costs,” The Quarterly Review of Economics and Finance, vol. 50, no. 2, pp. 240–243, May 2010, doi: 10.1016/j.qref.2009.12.005.
[101] P. Hernandez, X. Oregi, S. Longo, and M. Cellura, “Life-Cycle Assessment of Buildings,” in Handbook of Energy Efficiency in Buildings, Elsevier, 2019, pp. 207–261.
[102] E. W. McAllister, “Economics,” in Pipeline Rules of Thumb Handbook, Elsevier, 2014, pp. 673–721.
[103] E. R. Yescombe, “What is Project Finance?,” in Principles of Project Finance, Elsevier, 2014, pp. 5–27.
[104] “Corporate Tax Guide.” Lesotho Revenue Authority, 2017, Accessed: Oct. 29, 2019. [Online]. Available: http://www.lra.org.ls/sites/default/files/201705/Corporate%20Tax%20Guide.pdf.